



Measuring antimicrobial efficacy against sulfate-reducing bacterial biofilms
by Lawrence Robert Gardner

A thesis submitted in partial fulfillment of the requirements for the degree of Master of Science in
Chemical Engineering
Montana State University
© Copyright by Lawrence Robert Gardner (1999)

Abstract:

A laboratory reactor system was used to measure the efficacy of glutaraldehyde and nitrite treatments in controlling sulfide generation by sulfate-reducing bacterial biofilms. The experimental system consisted of an annular reactor inoculated with an undefined mixed population from oilfield produced water and fed continuously with Postgate C medium. An anoxic environment and a temperature of 36°C were maintained in the reactor. Glutaraldehyde (500 mg/L, slug dose) and nitrite (100 mg-N/L, 24 h continuous feed dose) were administered to established sulfide-producing biofilms. Both treatments inhibited sulfide production. The glutaraldehyde treatment delayed recovery of sulfide generation (defined as the time required to attain 90 percent of pretreatment sulfide concentration) for an average of 73 h. Sulfide production began to recover within 2 to 4 h after the nitrite dosing was terminated and sulfide levels reached 90 percent of their steady-state values within approximately 24 to 32 h after the end of the dose. Both glutaraldehyde and nitrite penetrated the relatively thin biofilms (5 to 10 microns thick) readily. Biofilms recovered sulfide-generating capacity faster than planktonic cultures when treated with equivalent doses of glutaraldehyde. Corrosion of stainless steel reactor components was noted. Repeated doses of glutaraldehyde, on the same biofilm yielded similar results suggesting that adaptation of the biofilm in response to biocide treatment was not an important process in this case. While this laboratory system offers a reproducible approach to measuring antimicrobial efficacy against sulfate-reducing biofilms, an important outstanding question is how well it captures the performance of these treatments in the field.

MEASURING ANTIMICROBIAL EFFICACY AGAINST SULFATE-REDUCING
BACTERIAL BIOFILMS

by

Lawrence Robert Gardner

A thesis submitted in partial fulfillment
of the requirements for the degree

of

Master of Science

in

Chemical Engineering

MONTANA STATE UNIVERSITY-BOZEMAN
Bozeman, Montana

September 1999

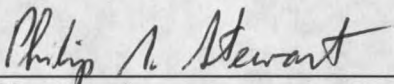
N378
G1745

APPROVAL

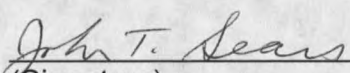
of a thesis submitted by

Lawrence Robert Gardner

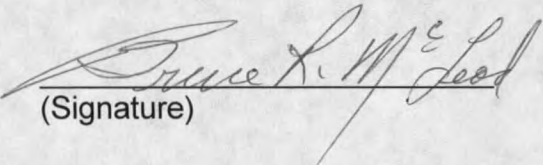
This thesis has been read by each member of the thesis committee and has been found to be satisfactory regarding content, English usage, format, citations, bibliographic style, and consistency, and is ready for submission to the College of Graduate Studies.

Dr. P. Stewart (Chair)	 _____ (Signature)	<u>9-9-99</u> Date
---------------------------	---	-----------------------

Approved for the Department of Chemical Engineering

Dr. J. Sears (Department Head)	 _____ (Signature)	<u>9-9-99</u> Date
-----------------------------------	---	-----------------------

Approved for the College of Graduate Studies

Dr. B. McLeod (Graduate Dean)	 _____ (Signature)	<u>9-9-99</u> Date
----------------------------------	--	-----------------------

STATEMENT OF PERMISSION TO USE

In presenting this thesis in partial fulfillment of the requirements for a master's degree at Montana State University-Bozeman, I agree that the Library shall make it available to borrowers under rules of the Library.

If I have indicated my intention to copyright this thesis by including a copyright notice page, copying is allowable only for scholarly purposes, consistent with "fair use" as prescribed in the U.S. Copyright Law. Requests for permission for extended quotation from or reproduction of this thesis in whole or in parts may be granted only by the copyright holder.

Signature Lawrence R. Gardner

Date September 9, 1999

ACKNOWLEDGEMENTS

I wish to extend my sincere appreciation to Philip Stewart, my research and academic advisor, for his invaluable guidance, financial support, and patience throughout this project. His direction, ideas, and consoling remarks were most appreciated when after eighteen months, we had to commence a new focus for the research program. I express gratitude to my committee members Gill Geesey and John Sears. Gill was instrumental in keeping the microbiological perspective alive with Dr. Sears guiding the way from the Chemical Engineering standpoint. A special thanks is extended to Nick Zelter for his efforts and assistance with our industrial associate sponsors of Amoco, Chevron, and Saudi Aramco.

I would like to thank all the students and staff members of the Center for Biofilm Engineering for enlightening my research, providing numerous extra-curricular distractions, and the friendships that I gained during my time in Bozeman. A extraordinary thank you goes to those individuals whom I have worked the closest with, namely the researchers of EPS 302 (Robin Gerlach, John Komlos, Andy Rice, and Chris Wend), and most notably our laboratory manager, John Neuman.

Finally and most importantly, I would like to thank my family, especially my wife, Sheri, for endless support, love, and encouragement during these demanding years.

TABLE OF CONTENTS

	Page
LIST OF TABLES	viii
LIST OF FIGURES	xiv
ABSTRACT	xix
INTRODUCTION	1
Background	1
Biofilm Formation and Heterogeneity	2
Biofilm Resistance to Antimicrobial Agents	5
Biofilm Control Strategies	7
Sulfate Reducing Bacteria in Oilfield Operations	9
Biofouling in the Petroleum Industry	10
Microbiologically Influenced Corrosion	12
Biofilm Control in the Petroleum Industry	14
Common Antimicrobial Agents	16
Alternative Sulfide Inhibition Strategies	18
Research Goal and Objectives	20
EXPERIMENTAL MATERIALS AND METHODS	21
Microorganisms	22
Enrichment and Inoculum Preservation	23
Planktonic Experiments	26
Biofilm Experiments	29
Annular Reactor Mixing Study	32
Annular Reactor Start-up and Operation	34
Biocide Addition	40
Nitrite Addition	41
Analytical Methods	41
Biofilm Sampling: Areal Carbon Density and Thickness	45
Enumeration with Epifluorescence Microscopy	46
RESULTS	50
Planktonic Experiments	50
Biofilm Experiments	54
Biofilm Reactor Mixing Characteristics	54
Sequence of Events for Biofilm Experiments	56

TABLE OF CONTENTS - Continued

	Page
RESULTS - <u>Continued</u>	
Control Experiments	59
Comparison of Control Experiments	60
Biocide Experiments	62
Glutaraldehyde and Control Dosing Comparison.....	64
Glutaraldehyde Reaction Rates	66
Nitrite Addition.....	71
Biofilm Coupon Analyses.....	76
Biofilm Thickness.....	76
Biofilm Areal Density.....	79
Microbiologically Influenced Corrosion	82
Transport Limitation.....	84
DISCUSSION	88
Experimental System.....	88
Planktonic – Biofilm Comparison	90
Equivalent Biocide Concentration	91
Relative Efficacy of Treatments	94
Comparison of Glutaraldehyde Efficiency – C^*t data	96
Biocide Penetration Analysis	100
Reaction of Glutaraldehyde with Biomass – Annular Reactor versus Pipeline	101
Recommendations for Future Work.....	104
CONCLUSIONS	106
REFERENCES CITED	107
APPENDICES	116
APPENDIX A: Biofilm Reactor Specifications.....	117
APPENDIX B: Analysis of Annular Reactor Mixing Characteristics	125
APPENDIX C: Experimental Data for Hydraulic Mixing Study	131
APPENDIX D: Standard Curves	155
APPENDIX E: Planktonic Experimental Data	159
APPENDIX F: Biofilm Experiment Data.....	170
APPENDIX G: Biofilm Thickness Data.....	190
APPENDIX H: Total Organic Carbon Data	197
APPENDIX I: Planktonic and Biofilm Sulfide Recovery Time Data	204
APPENDIX J: Glutaraldehyde Dosing Data	209

TABLE OF CONTENTS - Continued

	Page
APPENDICES - <u>Continued</u>	
APPENDIX K: Effective Diffusivity Permeabilities in Water	218
APPENDIX L: Glutaraldehyde Inactivation Efficiency.....	222

LIST OF TABLES

	Page
Table 1. Medium Composition	23
Table 2. Annular Reactor Operating Conditions	30
Table 3. HP 5890 Series II Operating Conditions	44
Table 4. Planktonic recovery time in response to glutaraldehyde treatment. Recovery indices are expressed in terms of the time sulfide production is suppressed below 10 mg-S/L and the time required to reach 90% of steady-state sulfide levels. Recovery time was measured beginning at the time when fresh nutrients were supplied to the vials.....	53
Table 5. Hydraulic characteristics of non-reactive tracer studies.....	55
Table 6. Biofilm annular reactor biocide dosing sequence protocol	58
Table 7. Sulfate-reducing bacterial biofilm recovery time in response to glutaraldehyde treatments. Recovery indices are expressed in terms of the time sulfide production is suppressed below 10 mg-S/L and the time required to reach 90% of steady-state sulfide levels. Recovery time was measured beginning at the time when the nutrient amendment was reinitiated.	66
Table 8. Composite first-order reaction rate coefficients for the glutaraldehyde annular reactor experiments.....	68
Table 9. First-order reaction rate coefficients for the glutaraldehyde annular reactor experiments.....	70
Table 10. Sulfate-reducing bacterial biofilm recovery time in response to nitrite addition. Recovery indices are expressed in terms of the time sulfide production is suppressed below 10 mg-S/L and the time required to reach 90% of steady-state sulfide levels. Recovery time was measured beginning at the time when the nutrient amendment was reinitiated.	73
Table 11. Observable reaction rate for nitrite doses.....	76

LIST OF TABLES - Continued

	Page
Table 12. Biofilm thickness, L_f	77
Table 13. Biofilm areal density in terms of total organic carbon	80
Table 14. Effective Diffusive Permeabilities and Diffusion Coefficients	87
Table 15. Observable Moduli for glutaraldehyde and nitrite biofilm experiments.	87
Table 16. BST Model 920 Biofilm Annular Reactor Specifications.....	118
Table 17. Additional Apparatus Specifications	119
Table 18. Inner cylinder surface area calculation parameters.	120
Table 19. Outer cylinder surface area calculation parameters.	121
Table 20. Top plate surface area calculation parameters.....	122
Table 21. Bottom plate surface area calculation parameters.....	123
Table 22. Draft tube and coupon surface area calculation parameters.	124
Table 23. Hydraulic residence time analysis notation.....	129
Table 24. Hydraulic residence time analysis for biofilm tracer studies.	130
Table 25. Computational analysis for a bottom fed non-reactive tracer (Tracer #1, $\omega = 230$ rpm).....	132
Table 26. Computational analysis for a bottom fed non-reactive tracer (Tracer #2, $\omega = 230$ rpm).....	133
Table 27. Experimental data and computation for a bottom fed non-reactive tracer (Tracer #3, $\omega = 150$ rpm).....	134
Table 28. Computational analysis for a bottom fed non-reactive tracer (Tracer #3, $\omega = 150$ rpm).....	142

LIST OF TABLES - Continued

	Page
Table 29. Linear regression summary for the natural logarithm transformation of the concentration versus time data (Tracer #3, $\omega = 150$ rpm).....	143
Table 30. Experimental data and computation for a bottom fed non-reactive tracer (Tracer #4, $\omega = 150$ rpm).....	144
Table 31. Computational analysis for a bottom fed non-reactive tracer (Tracer #4, $\omega = 150$ rpm).....	153
Table 32. Linear regression summary for the natural logarithm transformation of the concentration versus time data (Tracer #4, $\omega = 150$ rpm).....	154
Table 33. January 7, 1998 batch vial data.....	160
Table 34. November 18, 1998 batch vial data.....	161
Table 35. March 18, 1999 batch vial data.....	162
Table 36. Planktonic Experiment #1 – Control	163
Table 37. Planktonic Experiment #1 – 50 mg/L glutaraldehyde.....	163
Table 38. Planktonic Experiment #1 – 100 mg/L glutaraldehyde.....	164
Table 39. Planktonic Experiment #1 – 350 mg/L glutaraldehyde.....	164
Table 40. Planktonic Experiment #1 – 500 mg/L glutaraldehyde.....	165
Table 41. Planktonic Experiment #2 – Control	166
Table 42. Planktonic Experiment #2 – 35 mg/L glutaraldehyde.....	166
Table 43. Planktonic Experiment #2 – 65 mg/L glutaraldehyde.....	167
Table 44. Planktonic Experiment #3 – Control	168
Table 45. Planktonic Experiment #3 – 35 mg/L glutaraldehyde.....	168

LIST OF TABLES - Continued

	Page
Table 46. Planktonic Experiment #3 – 65 mg/L glutaraldehyde.....	169
Table 47. Influent data for Control experiment #2 (Single dose of ultrapure water)	171
Table 48. Effluent data for Control experiment #2 (Single dose of ultrapure water)	172
Table 49. Influent data for Control experiment #3 (Repetitive dose of ultrapure water)	173
Table 50. Effluent data for Control experiment #3 (Repetitive dose of ultrapure water)	174
Table 51. Influent data for Dosing experiment #2 (Single dose of glutaraldehyde)	176
Table 52. Effluent data for Dosing experiment #2 (Single dose of glutaraldehyde)	177
Table 53. Influent data for Dosing experiment #4 (Repetitive dose of glutaraldehyde)	179
Table 54. Effluent sampling data for Dosing experiment #4 (Repetitive dose of glutaraldehyde)	180
Table 55. Influent sampling data for Dosing experiment #6 (Repetitive dose of nitrite)	182
Table 56. Effluent sampling data for Dosing experiment #6 (Repetitive dose of nitrite)	183
Table 57. Influent sampling data for Dosing experiment #8 (Repetitive dose of glutaraldehyde)	186
Table 58. Effluent sampling data for Dosing experiment #8 (Repetitive dose of glutaraldehyde)	187
Table 59. Biofilm thickness data for Control #2	191

LIST OF TABLES - Continued

	Page
Table 60. Biofilm Thickness Data for Control #3.	192
Table 61. Biofilm Thickness Data for Experiment #2.	193
Table 62. Biofilm Thickness Data for Experiment #4.	194
Table 63. Biofilm Thickness Data for Experiment #6.	195
Table 64. Biofilm Thickness Data for Experiment #8.	196
Table 65. Total organic carbon and areal density data for Control #2.	198
Table 66. Total organic carbon and areal density data for Control #3.	199
Table 67. Total organic carbon and areal density data for Experiment #2.	200
Table 68. Total organic carbon and areal density data for Experiment #4.	201
Table 69. Total organic carbon and areal density data for Experiment #6.	202
Table 70. Total organic carbon and areal density data for Experiment #8.	203
Table 71. Planktonic sulfide recovery times to achieve 10 mg S/L and 90% of steady-state.	205
Table 72. Biofilm sulfide recovery times to achieve 10 mg S/L and 90% of steady-state.	207
Table 73. Glutaraldehyde concentration versus time data for Experiment #2.	210
Table 74. Experiment #2 linear regression summary for the natural logarithm transformation of the glutaraldehyde concentration versus time data.	211
Table 75. Glutaraldehyde concentration vs. time data for Experiment #4 Dose #1.	212
Table 76. Glutaraldehyde concentration vs. time data for Experiment #4 Dose #2.	213

LIST OF TABLES - Continued

	Page
Table 77. Experiment #4 linear regression summary for the natural logarithm transformation of the glutaraldehyde concentration versus time data.....	214
Table 78. Glutaraldehyde concentration vs. time data for Experiment #8 Dose #1.....	215
Table 79. Glutaraldehyde concentration vs. time data for Experiment #8 Dose #2.....	216
Table 80. Experiment #4 linear regression summary for the natural logarithm transformation of the glutaraldehyde concentration versus time data.....	217
Table 81. Wilke-Chang effective diffusive permeability parameters	220
Table 82. Inactivation efficiency for different disinfection concentrations	223

LIST OF FIGURES

	Page
Figure 1. BioSurface Technologies Model 920 biofilm annular reactor	31
Figure 2. Hydraulic residence time tracer study schematic	33
Figure 3. Schematic of biofilm annular reactor experimental system	38
Figure 4. Photo of biofilm annular reactor laboratory system	39
Figure 5: Diagram of cryoembedding and cryosectioning procedures.	48
Figure 6. Sulfide production and sulfate uptake for a planktonic suspension enriched with Postgate C medium at 36°C (November 18, 1998 data).	51
Figure 7. Effect of glutaraldehyde on the activity of planktonic sulfate- reducing bacteria. (Planktonic Experiment #1).....	52
Figure 8. Effluent concentration profile from Tracer #3 for a bottom feed to the annular reactor. The reactor was operated at 150 rpm with an influent flow rate of 7.9 mL/min.	55
Figure 9. Washout behavior (slope = dilution rate, <i>D</i>) of the non-reactive tracer in the BST Model 920 biofilm annular reactor.	56
Figure 10. Sequence of events during a biofilm experiment (Experiment #8). The numbers correspond to the steps summarized in Table 6.	58
Figure 11. Typical annular reactor control experiment. Concentration profiles for sulfide and sulfate in response to a repetitive dose with ultrapure water. See Table 6 and Figure 10 for experimental protocol. (Control #3 data)	59

LIST OF FIGURES - Continued

	Page
Figure 12. Sulfide and sulfate profile comparison for annular reactor control experiments administered with a 1-mL dose of ultrapure water. The notation #1 implies dose #1 and #2, dose #2. Time zero denotes the pulse injection of ultrapure water; <i>-6.5hr</i> the time nutrient amendment ceased; and <i>+7hr</i> the time nutrient amendment was reinitiated.	61
Figure 13. Sulfide and sulfate concentration profiles in response to repetitive pulse injections of 500 mg/L glutaraldehyde. See Table 6 and Figure 10 for experimental protocol. (Annular reactor Experiment #8 data).....	63
Figure 14. Sulfide profile comparison for three separate annular reactor experiments that were subjected to a single dose of 500 mg/L glutaraldehyde. Time zero denotes the pulse injection of glutaraldehyde; <i>-6.5hr</i> the nutrient ceased; and <i>+7hr</i> was reinitiated.	63
Figure 15. Sulfide profile comparison between a control experiment with ultrapure water versus a dose of 500 mg/L glutaraldehyde. Time zero denotes the pulse injection of glutaraldehyde; <i>-6.5hr</i> the time nutrient amendment ceased; and <i>+7hr</i> the time nutrient amendment was reinitiated. (Annular reactor data from Control #3 and Experiment #2)	65
Figure 16. Natural logarithm of the glutaraldehyde concentration versus time for all glutaraldehyde annular reactor experiments. The slope of these curves provides the first order reaction rate coefficients of the glutaraldehyde.....	68
Figure 17. Sulfide and sulfate concentration profiles in response to two 24-hour continuous feeds of 110 mg-N/L of nitrite. See Table 6 and Figure 10 for experimental protocol. (Annular reactor Experiment #6 data).....	72
Figure 18. Comparison of nitrite and glutaraldehyde washout profiles from the biofilm annular reactor.....	74

LIST OF FIGURES - Continued

	Page
Figure 19. Natural logarithm of nitrite concentration versus time for two separate doses in annular reactor Experiment #6. The slope of these curves provides the first-order reaction rate coefficients during washout.....	74
Figure 20. Progression of the average biofilm thickness during the annular reactor experiments. The acronyms imply dosing intervals, e.g. SS1 = Steady-State #1, AD1 = After Dose #1, etc. Control #2 and Experiment #2 were single dose studies while the remaining experiments experienced repetitive doses. Control experiments were subjected to dosing with ultrapure water. Experiments #2,4 and 8 were glutaraldehyde studies while Experiment #6 addressed the effects of nitrite addition.....	78
Figure 21. Changes in areal carbon density as a function of dosing interval during a biofilm experiment. The acronyms imply these intervals, e.g. SS1 = Steady-State #1, AD1 = After Dose #1, etc. Control #2 and Experiment #2 were single dose studies while the remaining experiments experienced repetitive doses. Control experiments were subjected to dosing with ultrapure water. Experiments #2,4 and 8 were glutaraldehyde studies while Experiment #6 addressed the effects of nitrite addition.	81
Figure 22. Stub shaft and bearing from the bottom plate of the biofilm annular reactor. Damages to these surfaces by the sulfate-reducing bacteria generated corrosion by-products are evident by the scored and blackened surfaces. A clean shaft and bearing are shown for comparison.....	83
Figure 23. Microbially influenced corrosion by sulfate-reducing bacteria on the bottom plate stub shaft. This shaft was extracted after 17 days in the biofilm reactor.	85

LIST OF FIGURES - Continued

	Page
Figure 24. Comparison of microbial sulfide production recovery time as a result of biocide treatment. Recovery indices are expressed in terms of the time sulfide production is suppressed below 10 mg-S/L and the time required to reach 90% of steady-state sulfide levels. Recovery time was measured beginning at the time when the nutrient amendment was reinitiated.	93
Figure 25. Comparison of inactivation efficiency at different disinfection concentrations. (Eagar: <i>P.fluorescens</i> ; Cheung & Beech #2: Portsmouth Harbor SRB; Cheung & Beech #2: Indonesian coast SRB; Grab & Theis #1: <i>D.desulfuricans</i> ; Grab & Theis #2: Prudhoe Bay SRB isolate; Ruseska: undefined SRB population; Our Work: undefined SRB population)	98
Figure 26. Effluent tracer concentration profile for Tracer #1 ($\omega = 230$ rpm). A 1-mL pulse injection of red food coloring with absorbance levels recorded at $\lambda = 470$ nm.	132
Figure 27. Effluent tracer concentration profile for Tracer #2 ($\omega = 230$ rpm). A 1-mL pulse injection of red food coloring with absorbance levels recorded at $\lambda = 500$ nm.	133
Figure 28. Effluent tracer concentration profile for Tracer #3 ($\omega = 150$ rpm). A 1-mL pulse injection of red food coloring with absorbance levels recorded at $\lambda = 500$ nm.	142
Figure 29. Effluent tracer concentration profile for Tracer #4 ($\omega = 150$ rpm). A 1-mL pulse injection of red food coloring with absorbance levels recorded at $\lambda = 500$ nm.	153
Figure 30. Hydrogen sulfide standard curves used in calculating sulfide levels during the planktonic and biofilm experiments.	156
Figure 31. Glutaraldehyde standard curves used in the analysis of biocide levels during the planktonic and biofilm experiments.	157
Figure 32. Nitrite standard curve. This linear relationship was utilized to determine nitrite concentration levels during Experiment #6.	158

LIST OF FIGURES - Continued

	Page
Figure 33. January 7, 1998 batch vial enrichment. Sulfate and sulfide profiles during a 36-hour growth cycle with change in sulfide concentration versus change in sulfate concentration.....	160
Figure 34. November 18, 1998 batch vial enrichment. Sulfate and sulfide profiles during a 36-hour growth cycle with change in sulfide concentration versus change in sulfate concentration.....	161
Figure 35. March 18, 1999 batch vial enrichment. Sulfate and sulfide profiles during a 36-hour growth cycle with change in sulfide concentration versus change in sulfate concentration.....	162
Figure 36. Planktonic Experiment #1. Sulfide recovery profiles in response to varying concentrations of glutaraldehyde.....	165
Figure 37. Planktonic Experiment #2. Sulfide recovery profiles in response to varying concentrations of glutaraldehyde.....	167
Figure 38. Planktonic Experiment #3. Sulfide recovery profiles in response to varying concentrations of glutaraldehyde.....	169
Figure 39. Experiment #2. Glutaraldehyde first-order rate coefficient determination.	210
Figure 40. Experiment #4 Dose #1. Glutaraldehyde first-order rate coefficient determination.	212
Figure 41. Experiment #4 Dose #2. Glutaraldehyde first-order rate coefficient determination.	213
Figure 42. Experiment #8 Dose #1. Glutaraldehyde first-order rate coefficient determination.	215
Figure 43. Experiment #8 Dose #2. Glutaraldehyde first-order rate coefficient determination.	216

ABSTRACT

A laboratory reactor system was used to measure the efficacy of glutaraldehyde and nitrite treatments in controlling sulfide generation by sulfate-reducing bacterial biofilms. The experimental system consisted of an annular reactor inoculated with an undefined mixed population from oilfield produced water and fed continuously with Postgate C medium. An anoxic environment and a temperature of 36°C were maintained in the reactor. Glutaraldehyde (500 mg/L, slug dose) and nitrite (100 mg-N/L, 24 h continuous feed dose) were administered to established sulfide-producing biofilms. Both treatments inhibited sulfide production. The glutaraldehyde treatment delayed recovery of sulfide generation (defined as the time required to attain 90 percent of pretreatment sulfide concentration) for an average of 73 h. Sulfide production began to recover within 2 to 4 h after the nitrite dosing was terminated and sulfide levels reached 90 percent of their steady-state values within approximately 24 to 32 h after the end of the dose. Both glutaraldehyde and nitrite penetrated the relatively thin biofilms (5 to 10 microns thick) readily. Biofilms recovered sulfide-generating capacity faster than planktonic cultures when treated with equivalent doses of glutaraldehyde. Corrosion of stainless steel reactor components was noted. Repeated doses of glutaraldehyde, on the same biofilm yielded similar results suggesting that adaptation of the biofilm in response to biocide treatment was not an important process in this case. While this laboratory system offers a reproducible approach to measuring antimicrobial efficacy against sulfate-reducing biofilms, an important outstanding question is how well it captures the performance of these treatments in the field.

INTRODUCTION

Background

Biofilms consist of micro and macroorganisms that adhere to and populate a surface (Costerton *et al.*, 1995; Costerton, 1995; Fletcher, 1996). Microbial cells and abiotic substances are embedded in a protective extracellular polymeric matrix attached to a substratum (Characklis *et al.*, 1990) whose size, shape, and location are determined by species-specific factors (Costerton, 1995; Rice, 1999). These aquatic communities are continuously bathed with bulk fluid nutrients via interspersed water channels of the biofilm matrix. Biofilm formation confers protective and commensalistic effects for the participating organisms. Microorganisms in the biofilm mode of growth are less susceptible to deleterious chemical, physical and biological factors. Even when oligotrophic conditions persist, the biofilm matrix sequesters critical organic carbon and energy sources necessary for survival (Costerton and Lappin-Scott, 1995).

The ever-present microbial biofilm mode of growth was first observed by Geesey *et al.*, 1977. Biofilms are detrimental to many industrial and medical processes including: drinking water quality, souring of oil, corrosion of metals, reduced efficiency of heat-transfer equipment, increased drag of ships due to fouling of hulls, human infections, and medical implants (Costerton *et al.*, 1995).

Implanted devices are non-exempt from bacterial colonization with infection being the number one cause of failure. Some of the clinical related diseases and infections include cystic fibrosis (Doggett, 1969), coronary artery disease {Biomaterials Symposiums, 1998}, inner ear infections (Rayner *et al.*, 1998), prosthetic heart valves and joints {Biomaterials Symposium, 1998}, catheters, and pacemakers {Khardori, 1995; Biomaterials Symposium, 1998}

Biofilm Formation and Heterogeneity

The ubiquitous quality of bacterial biofilms is independent of the surface material, e.g. metals, inert materials, and human tissues. The topography of a given surface, however, dictates the pattern of the biofilm colonization (Camper *et al.*, 1994; Hamilton *et al.*, 1995; Scheuerman *et al.*, 1998). The first step in biofilm formation is the "conditioning" of the surface by the accretion of inorganic ions and organic molecules (Cheung and Beech, 1996; Costerton *et al.*, 1995; Marshall, 1996). This phenomenon results in the establishment of an organic film. Freely suspended organisms in the passing bulk fluid are then able to initiate colonization by adhering to these conditioned films. Depending on the environmental conditions, biofilm colonization may be driven by an affinity for specific adhesion receptors, e.g. substrates, proteins, or even the surface material.

Direct observation via various forms of microscopy has enabled researchers to capture the majority of what we know about microbial biofilms. Coupling of microprobes with confocal scanning laser microscopy (CSLM), has illuminated a

more definitive snapshot of the intrinsic complexity, sophistication, and heterogeneity of bacterial biofilms through three-dimensional images and time-lapse photography (Costerton, 1995; Dalton *et al.*, 1994; Lawrence *et al.*, 1991; Lewandowski *et al.*, 1993; de Beer *et al.*, 1994). The term "biofilm" implies an encapsulated matrix of microorganisms protected from environmental stresses with the constitutive ability to adapt to adverse changes in their habitat. Biofilm cells are protected by a microbially produced layer of extracellular polymeric substances (EPS). The layer is composed of polysaccharides, proteins and other organic matter. The EPS matrix may aid in the protection from biocidal activity in the form of diffusional resistance (Stoodley *et al.*, 1994).

The initial planktonic cells that colonize a surface undergo a phenotypic transformation to a sessile state and in turn function as the parent population of the resulting biofilm. There is an apparent lag time in the subsequent replication associated with the attachment event (Rice, 1999). It has been speculated that during this lag phase in growth, the cells are increasing EPS production and switching to a biofilm phenotype, by inducing new genes. The progeny or daughter cells of the parent organisms have the ability to redistribute along the surface, establish dense colonies near the parent cells, detach into the bulk liquid, or form long chains of cells (Lawrence and Caldwell, 1987; Power and Marshall, 1988; Rice, 1999). In the case of a *Pseudomonas aeruginosa* PA01 strain, Rice (1999) observed that some replicated cells moved away from their original locations and subsequently colonized new regions of the surface.

A major difference between planktonic and biofilm mode of growth is the critical role of nutrient transfer to the adherent populations. Biofilms are often limited by the mass transport of available nutrients, which results in a concentration gradient from the bulk liquid to the underlying substratum. Just as the EPS provided a barrier to unwanted biocides, this layer can also diminish the nutrients necessary to the microorganisms deep within the biofilm structure. There are three potential avenues of obstruction to nutrient delivery: external mass transport from the bulk liquid to biofilm interface (Characklis *et al.*, 1990), diffusion into the biofilm (Hoyle *et al.*, 1993), and potential reaction with biofilm constituents prior to reaching the substratum. With the upper layers of the biofilm being readily accessible to passing nutrients, it has been proposed that the cells closer to the surface are actively growing while the organisms deeper into the structure are less active (Huang *et al.*, 1998; Wentland *et al.*, 1996). Inherent heterogeneity of the biofilm was confirmed by decreasing concentration profiles of metabolic substrates, oxygen (Stoodley *et al.*, 1994), biocides (Sanderson and Stewart, 1997), and tracers (Reinsel, 1995). In some cases, the diffusion profiles illustrated regions of limited permeability, i.e. water channels, followed by areas of transport limitation (Lewandowski *et al.*, 1993). However, metabolic cooperation between different microbial species, where the by-product of one species is a nutrient source for another species, may be an important aspect of natural biofilm growth (Costerton, 1995; MacLeod *et al.*, 1990)

Heterogeneity within biofilms has been traditionally documented with regards to

the chemical and structural aspects of the biofilm (de Beer *et al.*, 1994; Stoodley *et al.*, 1994). Little *et al.* 1987 acknowledged the existence of an electrical gradient between adjacent cells that manifested into a measurable corrosion potential for a conductive surface. Costerton *et al.* (1994) found electrical potentials were present regardless of the colonized surface conductivity. The corresponding movement of ions and charged molecules is dictated by this gradient which may impede the ability of charged biocides and antibiotics to diffuse into the biofilm matrix. Modification to the biofilm electrical potential by an externally applied electric field, termed the bioelectric effect (Costerton *et al.*, 1994), was shown to enhance the efficacy of antibiotics when used against a biofilm.

Biofilm Resistance to Antimicrobial Agents

It has been widely reported that biofilms possess a higher degree of resistance to antimicrobial agents (Cochran *et al.*, 1998; Characklis *et al.*, 1990; Chen *et al.*, 1993; de Beer *et al.*, 1994; Huang *et al.*, 1995; Sanderson and Stewart, 1997; Stewart, 1996; Srinivasan *et al.*, 1995; Xu *et al.*, 1995) when compared to their planktonic counterparts. There are four known mechanisms (Stewart *et al.*, 1998). These include, but are not limited to: (1) external mass transport from the bulk liquid to biofilm interface (Bott, 1992; Characklis *et al.*, 1990), (2) diffusion into the biofilm (Stewart, 1996; Stoodley *et al.*, 1994), (3) potential reaction or neutralization with constituents within the biofilm (Huang *et al.*, 1995; Sanderson and Stewart, 1997), and (4) physiological adaptation by the microorganisms

(Sanderson, 1996; Vransky *et al.*, 1997). Many antimicrobial agents that are tested under planktonic laboratory conditions have reduced effectiveness in field applications, where biofilms are predominant. Biocide concentrations that are effective against planktonic microorganisms tend to be less efficacious with bacterial biofilms due to the protective nature of the biofilm, EPS matrix, and physiological changes initiated by adverse conditions.

Antimicrobial delivery is quite different for suspended cultures compared to sessile populations. Planktonic organisms cannot escape the 360 degrees of exposed surface area whereas biofilm vulnerability is limited to the bulk liquid-biofilm interface. Antimicrobial delivery into a biofilm is actually a complex process. The delivery of the biocide must first overcome external mass transfer resistance. This reduces the biocide concentration at the biofilm interface relative to the bulk fluid concentration. The antimicrobial agent must then diffuse into the biofilm where it reacts with and is neutralized by components of the biofilm, resulting in further reductions in concentration (Gilbert *et al.*, 1990). De Beer *et al.* (1994) used a chlorine microelectrode and found chlorine concentration profiles within a binary species biofilm to be a function of chlorine levels and the neutralizing capacity of the biofilm matrix. In a similar fashion, Huang *et al.* (1995) documented a reduction in respiratory activity near the bulk liquid interface in response to a monochloramine dosing regime. Viability, however, was maintained adjacent to the substratum. The antibacterial activity of the monochloramine was diminished by the sacrificial layer of cells that were in close proximity with the bulk

fluid. This in turn resulted in a partial diffusion of the biocide and overall survival of the biofilm. Srinivasan *et al.* (1995) concluded that the decreased efficacy of monochloramine was attributed to transport limitations for thick, robust biofilms but physiological changes were hypothesized as resistance mechanisms for thinner structures. The neutralization and physiological responses by bacterial biofilms in response to monochloramine was further substantiated by the work of Sanderson and Stewart (1997). A phenomenological model was applied to a repetitive dosing regime and predicted the overall trend in viable cells but overestimated the efficacy of the second dose. The researchers hypothesized a physiological adaptation by the *P. aeruginosa* biofilm to explain this discrepancy.

Biofilm Control Strategies

While biofilms possess appealing qualities in the areas of wastewater management and biodegradation of toxic chemicals, the majority of biofilm awareness or research has been concentrated toward eradication of these structures. The economic impact coupled with health related issues are staggering. Control and/or removal of bacterial biofilms is (are) an overwhelming assignment. Historical approaches to dealing with unwanted biofilms have utilized mechanical and/or chemical therapies. Mechanical approaches are often expensive and difficult to implement due to limited accessibility of the fouled surfaces, whereas chemical treatments are universal in their delivery. Chemical reagents are quite diverse in their modes of action ranging from broad-spectrum

disinfection with oxidizing biocides to tailored mechanisms of microbial disruption, such as compromised cell membrane integrity and interference with nucleic acid and protein synthesis. In the cost conscious markets of today's business world, the selection of a given product is often driven by economics.

System geometry factor plays a primary role in the effective administration of biocides. Accessibility of the biocide to all areas of a given environment is difficult to overcome. Biocides may not adequately penetrate crevices and populations within these crevices can therefore serve as an inoculum for biofilm re-growth (Bott, 1992).

Broad-spectrum agents are generally less expensive and non-specific towards individual organisms. Oxidizing compounds, such hypochlorous acid and monochloramine fall into this category (Boivin, 1995; Bott, 1992). Over the years, these antimicrobial agents have been a staple mode of treatment for the drinking water industry. While these agents were implemented to deter microbial activity, their interaction causes potential harmful effects to the delivery system via corrosion, toxic by-products, and associated odors. The chloramines, however, do not pose health risks and are less reactive when compared to free chlorine (Chen *et al.*, 1993; Chen *et al.*, 1994; LeChevallier *et al.*, 1988). Monochloramine's less reactive nature imparts longer lasting residuals and was more effective than free chlorine for inactivation of *P. aeruginosa* biofilms (Chen *et al.*, 1993; Griebe *et al.*, 1994).

Antimicrobial agents are applied into the bulk fluid in one of two ways: pulse injection (slug treatment) or a continuous dose for a specific period of time. The manner in which a biocide is applied to a system greatly influences how well the biocide will perform in that system. Slug treatments have been documented to provide a more cost effective and efficacious treatment as opposed to a continuous feed of low-levels of biocide (Dewar, 1986; McIlwaine, 1998). Antimicrobial agents control populations by killing or inhibiting bacterial metabolism but can also influence the dynamics of biofilm formation by reducing the initial adhesion of cells to surfaces. Biocide compounds change the surface free energy of a substratum by altering the conditioning layer. The modified surface may influence the number of microorganisms attaching to a surface. Since biocides alter cell wall integrity, adhesion of cells can either be promoted or inhibited due to changes of cell wall hydrophobicity (Cheung and Beech, 1996; Verran and Taylor, 1995).

Sulfate Reducing Bacteria in Oilfield Operations

Sulfate-reducing bacteria (SRB) are a group of phylogenetically diverse anaerobes which carry out dissimilatory reduction of sulfur containing compounds such as sulfate, sulfite, thiosulfate, and sulfur to sulfide (Bak and Cypionka, 1987; Lovley and Philips, 1994; Okabe *et al.*, 1994; Widdel, 1988). These organisms vary in their ability to influence metal deterioration (Cheung and Beech, 1996; Beech *et al.*, 1994). In the absence of sulfate or other inorganic electron

acceptors, some species of SRB can flourish by a fermentation pathway (Postgate, 1984). Sulfate-reducing bacteria metabolize a suite of organic compounds serving as electron donors. These compounds consist of hydrogen, lactate, pyruvate, the low molecular weight fatty acids of acetate, propionate, butyrate, etc. to the long chain fatty acids, keto acids, alcohols, and aromatic compounds (Postgate, 1984; Widdel, 1988). There are two primary nutritional classifications for sulfate-reducing bacteria. The first grouping conducts the incomplete oxidation of organic substrates to acetate while the second can completely oxidize the substrates to CO₂ (Okabe, 1992).

The activity of SRB in a number of natural and man-made systems is becoming more apparent and of economical concern (Bott, 1992; Grab and Theis, 1993). In particular, the oil and gas industries are seriously affected by the sulfides generated by SRB (Hamilton, 1994). Biogenic sulfide also poses health and safety problems, environmental hazards and severe economic losses due to corrosion of equipment (Odom and Singleton, 1992; Lee, 1990; Odom, 1990).

Biofouling in the Petroleum Industry

A subset of the detrimental effects caused by biofilm communities is the havoc rendered by sulfate-reducing bacterial biofilms in the petroleum industry. Biofilm accumulation in pipelines is of paramount importance to oilfield operations. Pipelines serve two primary objectives: transport of produced oil from the oilfield to refinery and secondary water injection into the oil-bearing formation to enhance oil

recovery (Bass *et al.*, 1998; Bass *et al.*, 1993; Herbert, 1994; Iverson and Olson, 1984; Lynch and Edyvean, 1988). The latter is the basis for this research.

Tardy-Jacquenod, *et al.* (1996) performed a study to determine the occurrence and metabolic capacity of sulfate-reducing bacteria from 14 different oilfield sites in France, the North Sea, and the Gulf of Guinea. This effort produced an isolation of thirty-seven sulfate-reducing bacteria strains: 16 from wellhead and 21 from pipeline operations. The results of their survey exemplify the ubiquitous nature of SRB populations in oil petroleum reservoirs and the problems faced with controlling their microbial activity.

Microbial activity by sulfate-reducing bacteria presents a foundation for multiple problems encountered in oilfield operations. These harmful effects include reservoir souring, decreased formation permeability, impeded secondary recovery operations, fouling of surfaces, and exacerbated corrosion. The technology for enhancing oil recovery has inadvertently increased down-hole microbial activity with a battery of field related problems. Sloughing of biomass contributes to the fouling of the reservoir by penetrating the porosity of the reservoir at a velocity front equivalent to the injected water (Rosnes *et al.*, 1991). SRB-mediated corrosion is a topic that has been extensively documented with links to localized corrosion, hydrogen induced cracking, stress corrosion cracking, corrosion fatigue (Hamilton, 1998; Lee *et al.*, 1995; Little and Wagner, 1994; Lynch and Edyvean, 1988). Corrosion in aqueous environments can be described as an electrochemical process that results in the destructive attack of metals. The significance and

extent of biocorrosion is readily apparent by the available literature devoted to corrosion by sulfate-reducing bacteria (Iverson and Olson, 1984). The existence of sulfidogens in biofilms attached to metal surfaces results in the initiation of corrosion due to the production of sulfide and organic acids (Bass *et al.*, 1998; Hamilton, 1985; Lee *et al.*, 1995).

Biofilm accumulation on the interior walls of the pipeline increases the fluid resistance with the potential for partially plugging the medium adjacent to the injection well. This results in restriction of flow (increased injection pressures or reduced injection rates) and as mentioned earlier, enhanced rates of corrosion. Previous work has shown a need for antimicrobial agents such as chlorine or glutaraldehyde in order to maintain biofilm activity and accumulation to a minimum (Cheung and Beech, 1996; Boivin, 1995; Vatsala and Mah, 1995; Grab and Theis, 1993; Whitham and Gilbert, 1993; Eagar *et al.*, 1988; Costerton and Lashen, 1983). The ramifications of sulfate-reducing bacteria respiration with respect to corroded surfaces are astronomical. While corrosion was not a monitored variable in this research, failure to mention this process would not present the complete picture of SRB activity in the field.

Microbiologically Influenced Corrosion

Corrosion is the naturally occurring electrochemical process by which materials fabricated of metal or their alloys undergo chemical oxidation from a ground state to an ionized species via two half-reactions: oxidation of the metal surface (the

anode), and the reduction of the chemical species (cathode) in contact with the metal. The oxidation products of a metal surface eventually serve as a diffusion barrier to further oxidation of the underlying metal. Changes in the environmental conditions can effect the stability of the protective metal oxide film and the susceptibility of the metal to corrosion (Scully, 1990). Microbiologically influenced corrosion (MIC) occurs when surface conditions are altered microbiologically via biochemical reactions. The resulting conditions prevail in the establishment and maintenance of the cathodic and anodic regions necessary for the promotion of corrosion (Stoecker II, 1995).

Bacterial influence on the corrosion of mild steel has been proposed by several models. Clearly, a number of factors are involved and not one predominant mechanism exists in the role of MIC by SRB's (Hamilton, 1998; Lee *et al.*, 1995). Cathodic depolarization refers to the anaerobic corrosion of ferrous metal by the removal of hydrogen, which is catalyzed by the presence of hydrogenase, and the production of iron sulfide (von Wolzogen Kuhr, 1934). The uptake of cathodic hydrogen comes at the expense of iron depletion at the anode. In a concerted fashion, the dissolution of iron reacts with bacterially produced sulfide generating a protective FeS film over the metal surface (Booth *et al.*, 1965). Ultimately the integrity of the film is compromised which exposes regions of unprotected and unreacted metal that can promote cathodic depolarization. Sulfide generation inhibits the formation of molecular hydrogen from atomic hydrogen thereby increasing the amount of atomic hydrogen at the metal surface and its deleterious

effects. Permeation of hydrogen into the metal structure causes embrittlement and stress cracking which are attributed to multiple types of failures in the petroleum industry. The ability to produce a broad spectrum of corrosive metabolic by-products over a wide range of environmental conditions makes bacteria a real threat to the stability of metals that have been engineered for corrosion resistance.

Biofilm Control in the Petroleum Industry

The choice and delivery of biocides to pipeline distribution systems in the petroleum industry are complex and often misunderstood. Early detection of microbiological activity is necessitated for a proactive approach in preventing the degradation of capital equipment and souring of oil. The physical characteristics of a pipeline vary in diameter, length, and material but possess one common characteristic, the lack of accessibility. This element impedes the field personnel's ability to assess and control microbial activity within the pipeline. Unfortunately, these inaccessible environments provide a "head start" for the proliferation of microbial communities on wall surfaces and in the oil-bearing formation. The presence and type of microbial activity is often difficult to detect, assess, and monitor. Another set of burdening factors are the time delay and available methodologies required in the assessment of biocide efficacy in controlling unwanted biofilms (Boivin, 1995; Eagar *et al.*, 1986; Herbert, 1994).

Ironically, the analysis of the inner surface of a pipeline yields approximately

1% of biotic material. The remaining material consists of inorganic scales, corrosion products, and entrained hydrocarbons. Accumulation of these bulk materials reduces the effective volume of the pipeline and increases the drag of the bulk liquid. Oil pipelines are one of the few aquatic environments with the affordable luxury to engage mechanical removal techniques with complimentary chemical strategies. In an attempt to remove the unwanted accumulation, the pipelines are routinely scraped by a process known as pigging. It is nearly impossible to entirely remove the deposits but the process disrupts the structures.

The incidence of reservoir souring has led to the deployment of combined chemical and physical strategies to diminish sulfate-reducing bacterial biofilms (Bass *et al.*, 1993; Herbert, 1994). Utilization of physical and chemical strategies, however, provides a contradictory situation for pipeline operations even though cleanliness of a pipeline and antimicrobial efficacy are inter-related. Physical removal of pipewall accumulation aids in the delivery of the antimicrobial to the actively respiring bacteria, but the removed debris can re-attach, proliferate, plug reservoirs, and potentially be more detrimental than long-term accumulation. The amount of solids removed by the mechanical operations provides a qualitative indication of system cleanliness. Although it is desirable to minimize the scraping events, the use of chemicals alone to mitigate microbial activity is cost prohibitive. Chemical agents are developed to impede microbial activity using different mechanisms of attack. In an attempt to make microorganisms more vulnerable to chemical strategies, some treatment programs have been developed by pooling

individual capabilities into a more synergistic effect, i.e. an agent that might disperse the biofilm is followed by another chemical that proves to be lethal to the microorganisms. A common theme to biofilm control is that methodologies and successes from one situation may not be easily extrapolated to another (Dewar, 1986).

Chemical treatment programs for field applications are initially established by vendor recommendations that were validated in laboratory and/or field trials. Determination of lethal biocide concentrations in the laboratory may fail to adequately capture the environmental and bacterial demands on the biocide (Dewar, 1986). Application of biocides in the field is hindered by a complex environment with the presence of oil droplets, corrosion by-products, and metal scrapings. Individually or in concert, these variables restrict the interaction of the biocide with the microorganisms (Whitham and Gilbert, 1993). The concentration of the biocide is intuitively important, but the surface area of the system in question and the reactivity of the reagent with biomass, other constituents, surfaces, etc. must also be considered.

Common Antimicrobial Agents

Control of biofilms and biocorrosion are frequently addressed by the delivery of chemical reagents. Glutaraldehyde (Scott and Gorman, 1991), isothiazolone (Gilbert *et al.*, 1990), formaldehyde (Rossmore and Sondossi, 1988), and halogenated biocides (LeChevallier *et al.*, 1988) have traditionally been used to

control microbial activity (Cheung and Beech, 1996). As mentioned above, biocides are broadly classified according to their chemical character, i.e. either oxidizing or non-oxidizing. Chlorine is by far the most widely used oxidizing biocide particularly in cooling water and drinking water distribution systems (Bott, 1992). Oxidizing biocides encompass a wide range of chemicals and environments (Boivin, 1995).

Another widely used group of organic compounds is the quaternary ammonium salts. These compounds possess a cationic charge, which binds with the negatively charged cell wall of the microorganism. Cell lysis results from the stresses associated with this electrostatic charge. Cell wall permeability is another mechanism of attack due to denaturing of cell wall proteins. While these compounds are rapidly biodegradable in low concentrations and are good bacteriostats, they are slow bactericides and expensive (Bott, 1992; Boivin, 1995; Lynch and Edyvean, 1988).

Application of aldehydes, e.g. glutaraldehyde and formaldehyde, to oilfield settings has been the basis of widely used treatment procedures. Glutaraldehyde has been used by itself or in combination with other biocides to increase its overall performance. The broad spectrum activity, nonionic nature, and tolerance to sulfide make glutaraldehyde an indispensable biocide for the petroleum industry. Major disadvantages of formaldehyde are potential carcinogenic effects, high doses required for effectiveness, and adaptation by microorganisms that offset its economical feature (Bessemers, 1983; Boivin, 1995).

Glutaraldehyde, 1,5-pentaedial, has been employed for nearly 30 years in an effort to control unwanted bacterial colonization in industrial systems. Gorman and Scott (1991) have outlined some of the plausible mechanisms responsible for the efficacy of glutaraldehyde with microorganisms. It is believed that the biocide interacts with the proteins of the outer cell membrane thereby diminishing the permeability of the cell (Dewar, 1986). This reduction in permeability hinders the transfer of nutrients and harmful by-products resulting in cell death (Cheung and Beech, 1996). As with any other biocide, the efficacy of glutaraldehyde is governed by the pH and temperature of the environment, contact time, and concentration. Eagar, *et al.* (1988) also suggested that the apparent efficacy of glutaraldehyde is the combined result of the chemical activity and the hydrodynamics of the environmental system. First, the microbial mode of attachment is partially compromised when subjected to the glutaraldehyde. This altered state then subjects the microorganisms to accelerated detachment by the abrading bulk fluid.

Alternative Sulfide Inhibition Strategies

Reservoir souring, the result of hydrogen sulfide production, has an enormous economic impact for oil companies at a cost of billions of dollars per year (Lee, 1990). In 1949, Allen noted the addition of nitrate to waste water was successful in controlling noxious sulfide odors and Jennemen (1986) favorably reported that nitrate inhibited sulfide production in a variety of anaerobic systems. Investigation

by researchers at Montana State University further determined that nitrate was being microbiologically reduced to nitrite (Mueller, 1994; Reinsel, 1995) and concluded that nitrite inhibited microbial souring. Comparisons between microbially reduced nitrite and external additions of nitrite yielded similar results. In a comparative study with glutaraldehyde, nitrite was found to be more effective at inhibiting sulfide production in sandstone columns (Goeres, 1995; Reinsel, 1995). Deployment of this alternative nitrite strategy reduces the environmental and economic concerns that commonly plague biocide delivery programs.

Research Goal and Objectives

A general purpose of the research presented in this thesis was to develop a working experimental system to evaluate the efficacy of biocides on a sulfate-reducing bacterial biofilm. Upon validation, the research objectives were more specifically tailored to address the following questions.

1. To what extent does transport limitation impede penetration of the biocide into the biofilm?
2. To what degree does the biofilm react with the biocide?
3. Does repetitive dosing with a non-oxidizing anti-microbial elicit an adaptive response?

EXPERIMENTAL MATERIALS AND METHODS

The goal of the experimental design was to enrich an undefined produced water sample while possessing conditions similar to an oilfield setting. Temperature, pH, and anoxic conditions were monitored and maintained during the experiments. An oxygen-free Postgate C medium with a 1.5% salinity level was utilized for enrichment, preservation, and experimental analysis. Water from a produced water facility was enriched for sulfate-reducing bacteria and used as the inoculum for the biocide efficacy studies.

The metabolic activity of these organisms was monitored by the production of sulfide as compared to the corresponding uptake of sulfate. The sulfide concentrations were determined by a modified methylene blue method (Cline, 1969) while the sulfate levels were measured via ion chromatography. Biomass was quantified by total organic carbon analysis with a biofilm thickness measurement determined by cryoembedding and cryosectioning procedures. The concentrations of glutaraldehyde were assayed by gas chromatography.

Microorganisms

Samples of produced water from the Chevron Lost Hills oilfield in California were used as the source of a microbial consortium for the planktonic and biofilm studies. A water analysis indicated low levels of carbon and energy sources available to the microorganisms although evidence of microbial colonization was apparent downstream. Produced water was aliquoted into four 1-L glass jars with oil added to the top of the containers to minimize aeration. Upon receipt in the laboratory, 200-mL of one of the 1-L containers was transferred in 50-mL aliquots to 100-mL sterile and anoxic vials. These vials and the remaining 1-L containers were stored at 40°F.

The growth culture medium for these sulfidogenic bacteria was a modified Postgate C medium (Postgate, 1984) with a 1.5% salinity level. The composition and concentrations are denoted in Table 1. The appropriate levels of the sodium sulfate and sodium dithionite solutions were obtained from Pfennig *et al.* (1986).

The Postgate C recipe provided a composite sulfate concentration of 1.024 g-S/L with a 60% (w/w) sodium lactate salt (Sigma-Aldrich *d/l*-lactic acid, L-1375) serving as the primary organic substrate.

Table 1. Medium Composition

Constituent	Concentration (g/L)
KH_2PO_4	0.5
NH_4Cl	1
Na_2SO_4	4.5
$\text{CaCl}_2 \cdot 6 \text{H}_2\text{O}$	0.06
$\text{MgSO}_4 \cdot 7 \text{H}_2\text{O}$	0.06
Sodium lactate	6
Yeast extract	1
$\text{FeSO}_4 \cdot 7 \text{H}_2\text{O}$	0.004
Sodium citrate $\cdot 2 \text{H}_2\text{O}$	0.3
NaCl	15
$\text{Na}_2\text{S} \cdot 9 \text{H}_2\text{O}$	3-mL of 2.5g/50-mL stock
Sodium dithionite ($\text{Na}_2\text{S}_2\text{O}_4$)	1-mL of a 1.5g/50-mL stock
0.1% Resazurin	1-mL

Enrichment and Inoculum Preservation

The base medium was prepared using the Hungate Method (Ljungdahl and Wiegel, 1986; Miller and Wolin, 1974) with the reducing agents of sodium sulfide and sodium dithionite. The sulfide solution was processed by adding 50-mL of ultrapure water to a 250-mL Corning Pyrex autoclavable media bottle (Fisher #06-414-1B) that incorporated a #6 size butyl-rubber stopper. The stopper was drilled to accommodate a Bellco anaerobic test tube (#2048-18150) equipped with a butyl rubber septum-type stopper and aluminum crimp ring. This facilitated anoxic and sterile transfers. While the headspace of the 250-mL bottle was being sparged

with high-purity nitrogen (99.99%), the sodium sulfide crystals were rinsed with ultrapure water to remove the inherent oxide layer, weighed, and quickly added to the bottle. The vessel was immediately sealed to limit any loss of sulfide to the gas phase. The high-purity nitrogen gas was introduced into a Lindberg/Blue M oven (Model #TF55035A) that contained a reducing column composed of copper wire maintained at 400°C. The gas was delivered to the appropriate vessels with an in-line 0.3 μm hydrophobic glass fiber bacterial air vent (Gelman Sciences #4210) and a sterile point-of-use 0.2 μm cellulose acetate syringe filter (Corning #21052-25). To further provide an anoxic environment, the sulfide bottle underwent a series of nitrogen and vacuum cycles via the rubber septum and a 25-ga. needle. This solution was subsequently autoclaved at 121°C for 30 minutes.

In a similar manner, the sodium dithionite solution was prepared by adding the appropriate amount of crystals to 50-mL of sterile oxygen-free ultrapure water in a 100-mL batch vial. The environment was made oxygen-free by performing the vacuum and nitrogen purge sequence three times. The final state of the vial headspace was maintained with a nitrogen positive pressure.

The 50-mL serum vials for enrichment and culturing were pre-assembled with a butyl rubber septum-type stopper and aluminum crimp ring followed by headspace evacuation with the nitrogen and vacuum sequence mentioned above. These vials remained under a state of vacuum prior to introduction with the medium.

To adequately provide an anoxic transfer of the Postgate C medium to the 50-mL serum vials, a 2-L Erlenmeyer flask was equipped with a butyl rubber stopper that included two process lines, one for a nitrogen purge and one for medium removal. The medium was boiled and cooled under a blanket of nitrogen per the Hungate method (Ljungdahl and Wiegel, 1986; Miller and Wolin, 1974). Once the medium cooled to room temperature, a positive pressure was supplied to the flask. Three-mL of the sodium sulfide and 1-mL of the 0.1% resazurin solutions were added to the mixture. Prior to these additions, the syringes were displaced of air via the high-purity nitrogen. A 60-mL syringe equipped with a 25-ga. needle was also purged with nitrogen prior to the aqueous transfers of the medium to the batch vials. The nitrogen blanket within the 2-L flask was periodically replenished as the headspace pressure diminished during the transfers.

Upon completion of the medium transfer, the individual batch vials were supplied with a nitrogen headspace and subsequently autoclaved for 30 min at 121°C. As the vials cooled to room temperature, 1-mL of filter-sterilized sodium dithionite was added to each vial. The pH of the base medium was initially adjusted to 8.0 using sterile 6N NaOH. This rendered a final pH = 7.0-7.5 (post sodium sulfide addition, autoclaving, and sodium dithionite addition). Periodic sampling of uncultured vials denoted a pH in the range of 7.2 to 7.3. The vials were stored at 40°F.

The initial enrichment of the preserved Lost Hills produced water was performed in duplicate. Vials were incubated at 35°C using a Lab-Line Imperial III

incubator, and assayed qualitatively via turbidity. Five-mL aliquots of these preserved produced waters were aseptically added to oxygen-free sterilized vials containing 30-mL of the modified Postgate C medium. As the vials became turbid, a sub-enrichment was prepared by transferring 1-mL to each of the five vials containing fresh Postgate C medium. It was during this portion of the culturing that the sulfate and microbially produced sulfide levels were monitored every two hours in an effort to capture a pseudo growth profile.

The resulting sulfide profile provided an optimum window of growth in which to perform the preservation of the inoculum. Hence, the frozen culture enrichments were permitted to grow into the mid to upper log phase prior to preservation with 20% (v/v) glycerol. The cryo-preservation vials were stored at -70°C . This enriched culture exhibited primarily Gram-negative staining. Motility and a curved rod-shaped morphology were noted under microscopic observation. Our population was not identified for specific sulfate-reducing bacteria even though other researchers have done so by 16S RNA methodologies (Amann *et al.*, 1991).

Planktonic Experiments

The efficacy of glutaraldehyde (the model biocide for our analysis and a benchmark in oilfield operations) for controlling suspended sulfate-reducing bacteria was determined in batch experiments using 50-mL batch vials. Various concentrations of the biocide were administered to determine a lethal dose for a

complete kill of planktonic organisms. The delivery of the biocide was designed to mimic the protocol for the annular reactor biofilm experiments (See Table 6 and Figure 10).

The biocide was administered in the late exponential to early stationary phase so that potentially toxic levels of sulfide did not inhibit the metabolism of the sulfate-reducing bacteria. In order to determine this optimum range, a confirmatory growth curve was generated to capture the metabolic activity of the microorganisms. Sulfide and sulfate levels were monitored over a 36-hour period.

For the biocide evaluation, the microorganisms were subjected to the dosing protocol as they entered the stationary phase. All portions of the protocol were carried out at 35°C. A 1.5-mL frozen culture was added to 30-mL of sterile and anoxic Postgate C media in a 50-mL batch vial. After approximately 30 hours (late exponential to early stationary phase), a 1-mL aliquot was transferred to a sterile, oxygen-free, and medium-free environment of 100-mL of 1.5% NaCl in a 250-mL Corning Pyrex autoclavable medium bottle equipped with a Bellco anaerobic test tube and butyl rubber septum-type stopper. The solution was incubated for a period of 6.5 hours. This time is analogous to the nutrient medium flush time in the biofilm experiments. At $t=6$ hours, the bottles were sampled for sulfide and sulfate. Upon completion of this "flush" stage, a 1-mL aliquot was transferred to 100-mL batch vials containing 60-mL of sterile and anoxic 1.5% NaCl at various glutaraldehyde concentrations, i.e. 0, 35, 50, 65, 100, 350, and 500 mg/L. The vials were incubated at 35°C for a period of 7 hours. The working concentrations

were made from a stock standard using the Union Carbide Uracide 250, a 50% (v/v), glutaraldehyde source.

At the end of the 7-hour contact period, the solutions were centrifuged to decant the unwanted aqueous component that contained the glutaraldehyde. A Sorvall Instruments Model RC5C centrifuge was operated at 10,000 rpm and 4°C for 10 minutes using the SS-34 rotor. The 60-mL centrifuge tubes were sparged with nitrogen for 5–10 minutes prior to sample transfer. Immediately after centrifuging and decanting the aqueous portion, a sterile and anoxic volume of 30-mL of Postgate C medium was added to re-suspend the pellet. The tube was vortexed for 2 minutes. These suspensions were then transferred to sterile and oxygen-free vials via a filter and syringe, which was followed by the addition of a nitrogen headspace. The ability of the planktonic sulfate-reducing bacteria to recover from the biocidal activity was quantified by sampling and analyzing the levels of sulfate and biogenic sulfide as they incubated at 35°C. The incubation period varied according to the biocide concentration and therefore ranged from 5 to 20 days. The "zero" concentration vial served as the control to the biocide treatments. This vial also accounted for any potential side effects as a result of the centrifugation and resuspension processes. In order to not deplete the available volume of nutrients within the vials, sulfate sampling did not occur until the sulfide concentration exceeded 10 mg S/L.

Biofilm Experiments

Assessment and screening of biocides has been educational and at times an overwhelming assignment. Early researchers performed screening operations using suspended organisms with the subsequent realization that the given concentrations were less effective in the field. Hence, the initial screening protocol was limited to batch vials with sessile efficacy evaluations being performed in laboratory pipeloops. While the laboratory loop was designed to mirror field criteria, its operation was cumbersome and time consuming. These combined qualities gave rise to the advent of smaller and quick turn around laboratory reactors, e.g. annular reactor, porous media columns, rotating disk reactors, and artificial biofilms (McIlwaine, 1998; Chen and Reinsel, 1996; Sanderson, 1996; Stewart *et al.*, 1998; Whitham and Gilbert, 1993; Pitts *et al.*, 1998).

A continuous flow annular reactor (BioSurface Technologies Corporation Inc., Model 920 with a digital rpm display) was chosen to evaluate the efficacy of glutaraldehyde for controlling sulfate-reducing bacteria. This type of reactor was selected due to a parallel but different study being performed by Chevron Inc. at their Lost Hills field site. The operating parameters listed in Table 2 mimic some of the field reactor configurations.

Table 2. Annular Reactor Operating Conditions

Parameter	Value	Units
Inner drum rotation	150	Rpm
Dilution rate	0.5	hr ⁻¹
Media flow rate	0.79	mL/min
1.5% NaCl flow rate	7.13	mL/min
Bulk liquid temperature	36	°C
Reactor volume	1	L
Nitrogen sparge flow rate @ 15 psi	6.1-8.6	mL/min

The BST Model 920 biofilm annular reactor consists of two concentric cylinders, a rotating inner cylinder and stationary outer cylinder. There is a provision for temperature control of the reactor environment via a water jacket adjacent to the stationary cylinder. Four vertical draft tubes on the inner cylinder ensures complete mixing of the reactor liquid phase. The annular reactor mixing characteristics were verified by a tracer study with the procedure listed in a forthcoming section. The rotating inner cylinder accommodates twenty removable coupon sites on the outer wall (Figure 1). Polycarbonate slides were used as the biofilm coupons. Each slide had an area of approximately 22 cm². The annular reactor provided an approximate wetted surface area to volume ratio of 260 m⁻¹. A detailed listing of the reactor component specifications is listed in Appendix A.

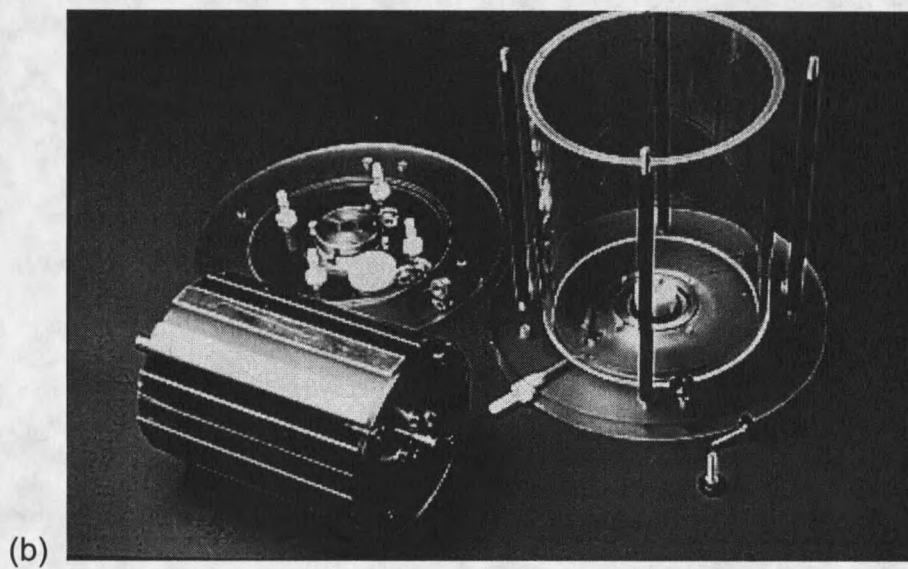
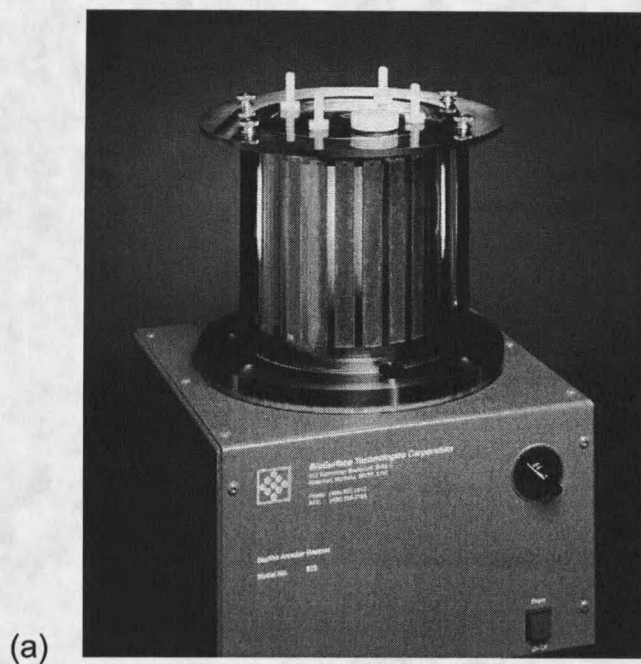


Figure 1. BioSurface Technologies Model 920 biofilm annular reactor

Annular Reactor Mixing Study

Prior to culturing a biofilm in the annular reactor, the reactor fluid residence time was characterized. A tracer study was performed with red food coloring to evaluate the mixing behavior within the reactor. The experimental setup is portrayed in Figure 2.

The effluent from the annular reactor was fed to the flow-through cell of a HACH DR2000 spectrophotometer. The distance between the effluent port and the spectrophotometer was minimized to alleviate any additional liquid volume and more importantly, to capture real-time changes within the reactor. Changes in the effluent concentration over time were recorded by downloading the absorbance readings via a RS232 cable (HACH #49670-00) to a Pentium®60 computer using HachLink data acquisition software (HACH #49665-00). This information provided an approximation to the hydraulic residence time distribution of non-reactive species moving through the reactor. The data ultimately aids in the interpretation of biocide reaction kinetics as the agents are displaced from the annular reactor.

Sampling intervals varied during the course of the experiment; every 10 seconds for the first 70 minutes followed by every minute for approximately 85 minutes, and then every 10 minutes for the remaining duration of the experiment, a period of 9 to 11 hours. The combined influent flow rate was set to 7.9 mL/min

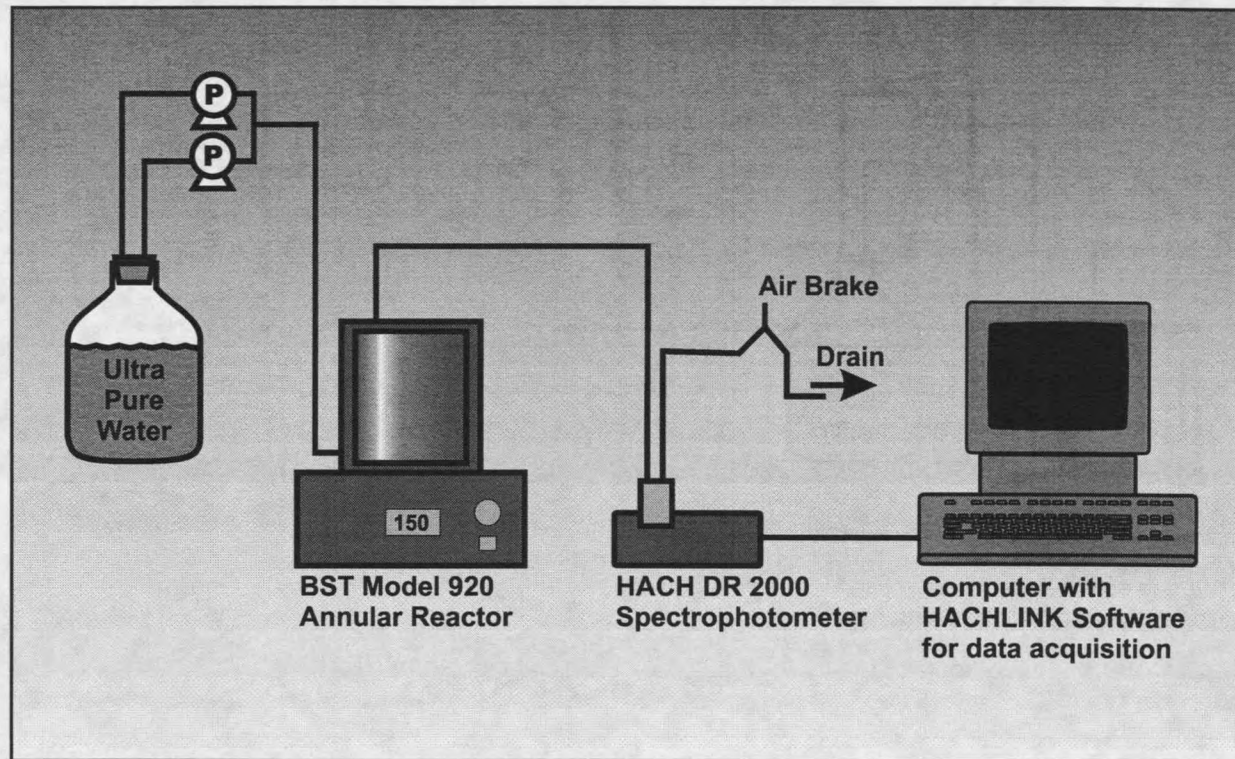


Figure 2. Hydraulic residence time tracer study schematic

using the medium and dilution water Masterflex feed pumps with the inner cylinder rotating at 150 rpm. The inlet was chosen to be at the bottom port of the reactor to eliminate the necessity for purging the reactor headspace during the anoxic experiments. The reactor was filled with approximately 1-L of deionized water and any entrained air was displaced with the aid of the feed water. A glass-Y serving as an air break was included on the downstream side of the flow-through cell to eliminate backpressure while providing a gravity feed to the drain. The maximum absorbance of the Schilling's red food coloring was determined by scanning the visible spectrum using a mixture comprised of one drop of the concentrated food coloring to 25-mL of deionized water. The maximum absorbance for this mixture was found to coincide at a wavelength of $\lambda = 500\text{nm}$. Data acquisition was initiated immediately prior to the 0.5-mL injection of the tracer at the inlet port.

Annular Reactor Start-up and Operation

The annular reactor and polycarbonate coupons were cleaned with hot water and a general-purpose laboratory tested cleaner (Fisherbrand Versa-Clean #04-343) followed by a cascading rinse with deionized water. Since an undefined oilfield inoculum served as our microbial consortium, the aseptic protocols were primarily confined to medium preparation and delivery. The focus of this effort was to eliminate contamination of the nutrient medium. Masterflex Tygon[®] food grade tubing (Cole-Palmer #06419) was used due to its durability upon autoclaving, transparency, and minimal gas permeability. A Masterflex Digital Console L/S

Drive (Cole-Palmer #07523-30) with Masterflex L/S size #13 tubing pump head (Cole-Palmer #07013-52) consisting of a polyphenylene sulfide housing and stainless steel rotor was used to deliver the medium to the reactor. A Masterflex Variable-Speed Console L/S Drive (Cole-Palmer #07521-50) and L/S size #16 tubing pump head (Cole-Palmer #07016-52) supplied the 1.5% NaCl solution. A glass flow break was included in the influent line to impede microbial migration from the biofilm reactor to the medium source. Process lines were pre-assembled and disinfected by pumping a 20 mg/L sodium hypochlorite solution for 10 minutes followed by a 2 hour rinse with sterile ultrapure water. It was during this period that the flow rates were verified and if necessary, adjusted accordingly. Once the reactor was filled with nutrient medium, an additional 3 hours of nutrient medium were processed through the reactor to counteract any residual sodium hypochlorite.

The Postgate C culture medium was prepared in 10-L quantities using a 13-L Pyrex[®] glass carboy. The initial annular reactor verification experiment included the sodium sulfide and sodium dithionite reducing agents. It was later determined that these constituents were unnecessary due to the intrinsic behavior of the mixed population in providing conditions favorable to the metabolism of sulfate-reducing bacteria. Henceforth, these reducing agents were no longer included.

The medium carboy was fitted with a butyl rubber stopper that accommodated ports for liquid transfer to the reactor, nitrogen sparging using a solvent reservoir filter (Waters #WAT025531), and a vent with an in-line 0.3 μm hydrophobic glass

fiber bacterial air vent (Gelman Sciences #4210). The delivery of high-purity nitrogen was set to 6.1-8.6 mL/min at 15 psi using a Cole-Palmer (#03216-04) flowmeter based upon dissolved oxygen levels. The pH of the medium was adjusted to 8.4-8.5 using sterile 6N NaOH and autoclaved for 3 hours at 121°C. Post-autoclaving, the medium was continuously purged with high-purity nitrogen to displace any absorbed oxygen during the cooling process. This purging sequence was maintained for a period of approximately 12 hours. A reducing column containing copper wire and maintained at 400°C removed traces of oxygen in the nitrogen feed. After cooling of the nutrient medium, aseptic and anoxic samples were obtained from the media for pH adjustment. The pH was adjusted to 7.1-7.3 using sterile 6 N NaOH via a syringe and 0.2 µm cellulose acetate syringe filter.

The 1.5% NaCl dilution water was prepared in 19-L quantities with ultrapure water using a 19-L Pyrex® glass carboy. The carboys were equipped in the same fashion as the medium containers. The solution was continuously mixed using a stir plate and purged with nitrogen for a 12-hour period prior to bringing the solution on-line. Oxygen levels were recorded using a CHEMet 0-1 ppm dissolved oxygen kit (Fisher Scientific #13-299-201).

Once the process lines were disinfected and flushed, the medium and dilution water carboys were placed on-line and used to fill the reactor with a 1/10 strength Postgate C medium (150-170 mg C/L and 102 mg S/L of sulfate). After filling the reactor, any entrained air was displaced with the continuous addition of the medium and dilution water. The flows were maintained for an additional 3 hours to

neutralize and/or flush any remaining reactive species of the disinfectant. The annular reactor was maintained at 36°C by means of a Neslab RTE-221 thermostat controlled water bath recirculating through the water jacket.

Aqueous samples from the rotating annular reactor were anoxically retrieved from the bulk liquid phase through a septum sampling port. The sampling port was fitted at the top of the reactor with a ¼" Teflon[®] male connector and 0.5" diameter Teflon[®] faced septum (Supelco#2-2657). In a similar fashion, a ¼" Teflon[®] union tee and septum was installed on the influent line. A sterile and reusable two-inch 22-ga. deflective noncoring septa penetration needle (Fisher Scientific #14-825-15L) was used to extract the sample. A schematic rendition and photograph as illustrated in Figures 3 and 4, respectively, depicts the experimental system.

Inoculation was accomplished by injecting 0.75-mL of a frozen stock culture into the reactor and letting it operate in batch mode for 2 hours. Continuous flow was then initiated to support the proliferation of aerobic organisms. The remaining 0.75-mL was used to inoculate a 30-mL Postgate C batch vial and enriched for approximately a 14-hour period. At this point, the reactor was returned to batch mode, inoculated with 30-mL of viable, sulfide-producing organisms and maintained for additional 48 hours. Sulfide levels rose to approximately 50 mg S/L during this time. Continuous flow was re-initiated at a flow rate of 7.9 mL/min. The influent process line and the bulk liquid phase were sampled for sulfate and sulfide. The polycarbonate biofilm coupons were systematically removed during

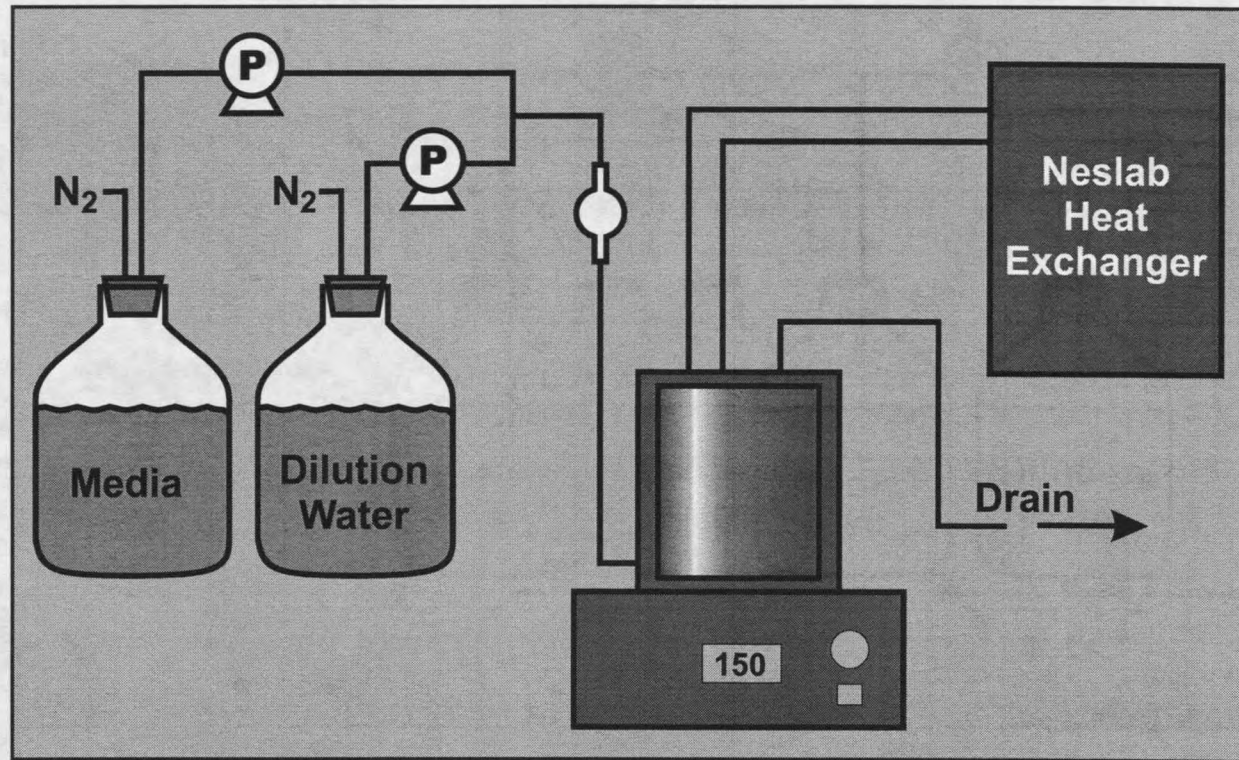


Figure 3. Schematic of biofilm annular reactor experimental system.



Figure 4. Photo of biofilm annular reactor laboratory system

the course of an experiment for the quantification of total organic carbon and biofilm thickness.

Biocide Addition

A series of batch vial experiments were performed at 35°C to investigate potential reactions of glutaraldehyde with the individual components of the nutrient medium. The glutaraldehyde was determined to be stable except in the presence of yeast extract. To prevent neutralization of glutaraldehyde by the nutrient medium, the Postgate C medium flow was turned off for 6.5 hours in advance of the biocide dose. The 1.5% NaCl dilution water continued to flow and displaced any residual medium from the reactor. A 1-mL dose of 50% glutaraldehyde was injected through the influent line to the 1-L reactor volume. A 1-mL sample from the bulk liquid was immediately taken for glutaraldehyde analysis. Sampling continued every 15 minutes for the next 7 hours. Approximately 0.6-mL of the sample was discarded as waste when it was filtered through a 0.2 µm cellulose acetate syringe filter. The remaining volume was filtered and dispensed into a 2-mL, 12 x 32 mm Target silanized screw thread vial (Fisher P/N 03-375-11AA or C4010-S2W). The concentration of glutaraldehyde was determined using a Hewlett-Packard 5890 Series II Gas Chromatograph. The flow of nutrient medium was reinstated at the completion of the 7-hour biocide treatment. Bulk liquid sulfate and sulfide concentrations were again monitored to capture the recovery of the sulfate-reducing bacteria.

Nitrite Addition

An additional biofilm study was performed in the annular reactor to investigate the effectiveness of nitrite as an inhibitor to biogenic sulfide by sulfate-reducing bacteria. A 24-hour continuous dose of approximately 110 mg N/L of sodium nitrite (VWR #SX0665-1, ACS grade) was delivered to the reactor. The nitrite solution was prepared anoxically in conjunction with the 1.5% NaCl dilution water. The flow of the nutrient medium was maintained to the reactor for the monitoring of metabolic activity. Nitrite levels were sampled from both the influent and bulk fluid ports with the latter at a frequency of every thirty minutes. Sulfide and sulfate concentrations were also obtained at these intervals. At the end of the 24-hour period, the nitrite/NaCl carboy was taken off-line and replaced with an anoxic carboy of 1.5% NaCl. Sampling continued as the nitrite was displaced from the reactor. Sulfide and sulfate levels were continually monitored to investigate any lasting suppression of sulfide generation by the sulfate-reducing bacteria.

Analytical Methods

Aqueous samples from the biofilm annular reactor were anoxically retrieved through a sampling port fitted with a 0.5" diameter Teflon[®] faced septum using sterile and reusable two-inch long 22-ga. deflective noncoring septum penetration needles and sterile syringes that were purged with nitrogen. Influent samples were

taken in a similar manner. A 1-mL sample was removed with 0.1 to 0.5 mL allotted for immediate sulfide analysis while the remaining volume was reserved for determination of sulfate concentration. If sampling point was to be performed in triplicate, three separate syringes were used to retrieve the samples.

While Rosser and Hamilton (1983) documented the simplicity of using a radiorespirometric assay in determining sulfate reduction (Maxwell and Hamilton, 1986; Rosser and Hamilton, 1983), sulfide concentrations were analyzed using the spectrophotometric assay described by Cline (1969). Once the sample was obtained from the annular reactor, it was immediately fixed in zinc acetate. In the case of a 50:1 dilution, the needle was immersed in 4.9-mL of 1% ZnAc and 0.1-mL of the sample was expelled into the solution. Five-mL of the 1% ZnAc served as the spectrophotometer blank. After the sample was placed in the zinc acetate to fix the soluble sulfide, 0.4-mL of the Diamine-R reagent was added and allowed to react for a minimum of 30 minutes. The absorbance was read at a wavelength of 670 nm using the Spectronic Instruments Genesys 5 Spectrophotometer.

The remaining 0.5-mL of the sample was diluted ten-fold with ultrapure water for determination of sulfate levels. These samples were stored in a freezer to inhibit metabolic activity until the sample could be processed. For sulfate analysis, the samples were pretreated with an OnGuard-Ag cartridge (Dionex #039637) in series with a 0.2 μm ion chromatography acrodisc (Fisher Scientific #09-730-257) due to the high levels of sodium chloride present in the samples. The 0.2 μm acrodisc was used to remove any suspended biomass. The first 2.5-mL from a 3-

mL aliquot were discarded post filtration with the remaining 0.5-mL dispensed into Dionex autosampler polyvials with filter caps (#38142). The samples were analyzed by ion chromatography using a Dionex IC DX300 configured with a 2-mm AS4A-SC anion column (#43125), a IonPac AG4A-SC guard column (#43126), and a 15 μ L sample loop. The mobile phase for the anion separation was a mixture of 1.7 mM sodium bicarbonate and 1.8 mM sodium carbonate delivered at 1 mL/min.

For the single nitrite experiment, nitrite levels were assessed using a spectrophotometric HACH Instruments Nitrite Test Kit (#20596-00). A 0.1-mL sample that was obtained with the same syringe for the sulfide and sulfate analyses was dispensed into 4.9-mL of ultrapure water. The HACH NitrVer 3 nitrite reagent pillow packet was added to the solution and vortexed for 1 minute. Absorbance readings were recorded at a wavelength of 546 nm using the Spectronic Instruments Genesys 5 Spectrophotometer. The absorbance values for the samples were consistently recorded ten minutes after adding the pillow packet due to a continuous reaction between the sample and the reagent. The samples were vortexed for an additional 50 seconds prior to the absorbance reading. Generation of the nitrite standard curve (Appendix D) was performed using an ACS grade of NaNO₂ with the same sample volumes listed above.

As mentioned in the Biocide Addition section, aqueous samples were also retrieved to assay for glutaraldehyde concentration by the means of gas chromatography. The reactor was sampled every 15 minutes for 7 hours (biocide

contact time). Filtered samples were immediately injected into the Hewlett-Packard 5890 Series II Gas Chromatograph that was equipped with a flame ionization detector (FID) and a 4ft. x 2mm ID glass packed column with 80/100 Porapak PS (Supelco P/N 2-0346). Three- μ L injections were made using a 10- μ L Hamilton Model 701 syringe (Alltech #803300). Some of the glutaraldehyde process parameters are listed in Table 3.

Glutaraldehyde standard curves were generated the day of treatment using a nominal 50% glutaraldehyde standard (1,5-pentanedial, Union Carbide). These curves are depicted in Appendix D.

Table 3. HP 5890 Series II Operating Conditions

Parameter	Value
Injector temperature	190°C
Detector temperature	250°C
Oven temperature	185°C
Column head pressure	33 psi
Carrier flow rate	20-21 ml/min
Helium pressure	60 psi
Air pressure	40 psi
Hydrogen pressure	20 psi
Detector type	FID
Run time	8 min

Biofilm Sampling: Areal Carbon Density and Thickness

Biofilm covered slides were removed through the threaded coupon port on top of the annular reactor. Sampling was performed by disinfecting this area with ethanol while flooding the port with a nitrogen blanket. The nutrient medium and dilution water flows were ceased with the influent and effluent lines pinched off. A screwdriver type of device fitted with a hook on the end was used to extract the polycarbonate coupons. Once a coupon was removed from the reactor environment, it was immediately replaced with a new one. Coupon selection throughout the different phases of an experiment was based upon a random number generator at the onset of the study. Care was taken to minimize the amount of time that the coupon port was open to the atmosphere. The retrieval and replacement of three coupons took approximately 2-3 minutes.

At least two coupons were sampled to determine biofilm carbon areal density. Upon removal, the coupons were individually placed into ~950-mL of sterile 1.5% NaCl for 5 minutes. This step was included to dilute any background carbon that might be associated with the nutrient medium as opposed to the intrinsic biomass carbon. Understandably, this protocol presents the opportunity for biofilm carbon loss. No sloughing of the biomass was observed during the rinsing step.

While carefully holding the coupon by the side edges, the biomass was scraped into a 100-mL beaker using a razor blade. The coupon was rinsed with 8-

mL of sterile 1.5% NaCl in 1-mL aliquots using a P1000 pipetman. Two additional milliliters were used to rinse the contents of the beaker into the dilution tube. The contents of the dilution tube were then homogenized for 1 minute with a Janke & Kunkel IKA-Labortechnik Ultra-Turrax T25 Homogenizer and an S25N-8G tip. The tip was autoclaved prior to use but flame sterilized and rinsed with ultrapure water between samples. For determination of total organic carbon, the samples were vortexed for 1 minute and processed using a Dohrman DC-80 Total Organic Carbon analyzer.

Enumeration with Epifluorescence Microscopy

Biofilm thickness was quantified by microscopic examination of frozen biofilm cross sections (Huang *et al.*, 1995; Yu *et al.*, 1994). The polycarbonate coupons were removed from the reactor by the same methodology described above and at the same interval as the areal carbon density coupons. As the coupon was removed from the annular reactor, it was turned on its edge to wick away any excess moisture. A layer of Tissue-Tek[®] O.C.T. Compound #4583 (10.24% w/w polyvinyl alcohol; 4.26% w/w polyethylene glycol; 85.5% w/w nonreactive ingredients) was placed on the lower and upper third portions of the coupon. The coupon was immediately placed on dry ice. Once the O.C.T. turned opaque white, which indicated solidification, the biofilm coupon was carefully flexed to remove the embedded specimen. The separated sample was then oriented with the substratum side up and placed back onto the dry ice with sterile tweezers.

Another layer of O.C.T. was added to cover this surface. When the specimen was fully encapsulated with the frozen O.C.T. matrix, the substratum was labeled with an indelible marker, wrapped in aluminum foil, and stored at -70°C prior to cryosectioning. The frozen biofilm sections were processed with the Leica CM 1800 Cryostat at a $5\ \mu\text{m}$ thickness and subsequently transferred to polylysine coated glass slides which possessed a positively charged surface (Fisher Scientific #12-550-17: 75mm x 25mm Colorfrost Plus microscope slides). Figure 5 illustrates the cryoembedding and cryosectioning procedures.

To effectively quantify biofilm thickness, the embedded sections were stained with a $1\ \mu\text{g}/\text{mL}$ concentration of DAPI (4', 6-diamidino-2-phenylindole) by dispensing $5\ \mu\text{l}$ drops with a RANIN EDP2 100 ml pipetman to cover the surface area of the sample. The slides were placed in the dark and air-dried for a period of 3 minutes. Tilting the slide on its side while adjacent to a laboratory napkin displaced the excess DAPI. Any residual stain was then carefully removed by blotting each section with Kimwipe tissue paper (Kimberly Clark, Fisher Scientific). The samples for all the experiments were stained on one occasion and stored at 40°F until microscopic examination.

The sectioned samples were examined using a Nikon Eclipse E800 microscope with epifluorescence illumination (100 watt mercury lamp). The microscope was equipped with a DAPI/UV cube unit with an excitation filter (340-380 nm) and a barrier filter (435-495 nm). Images were captured using a 40x oil

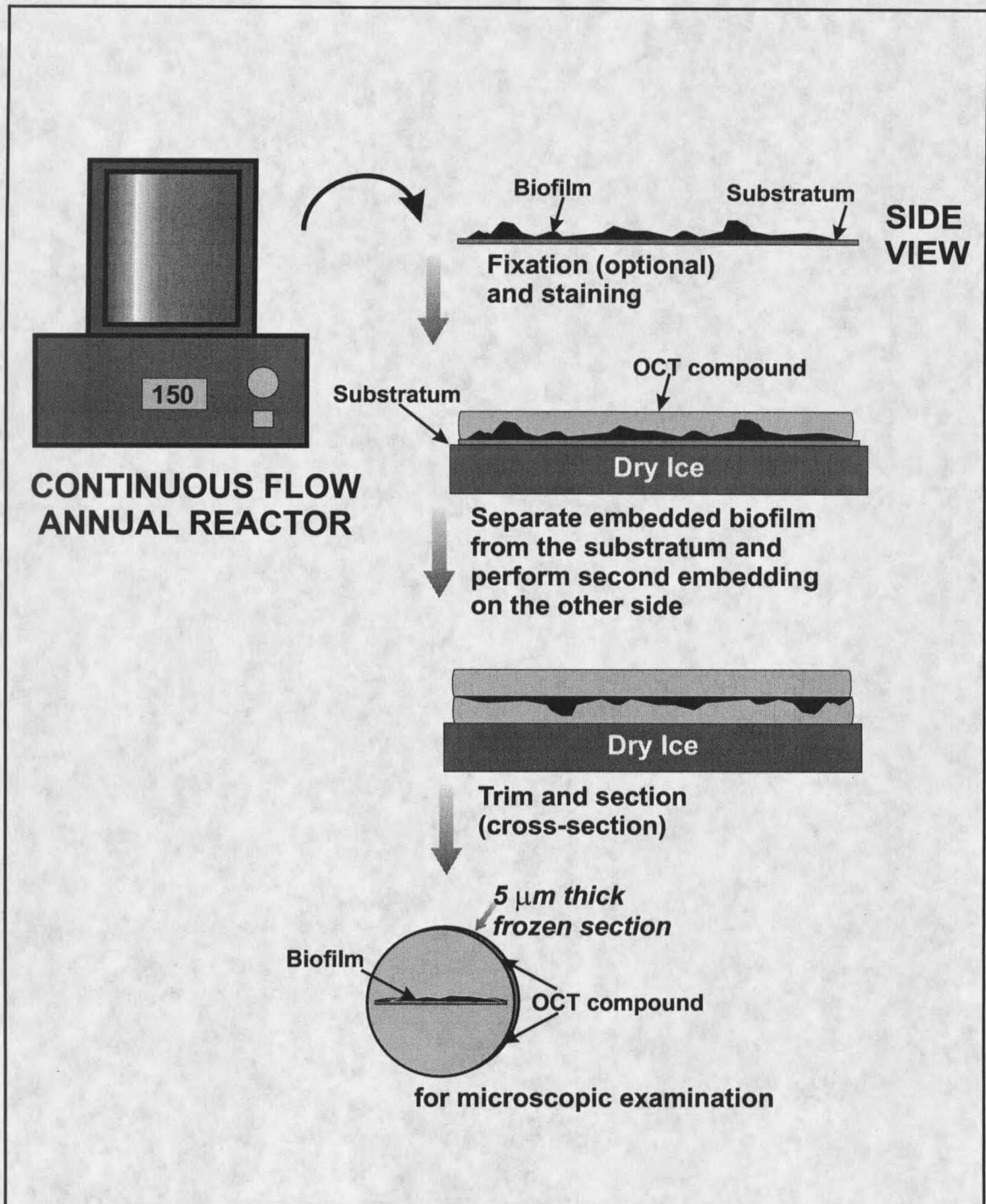


Figure 5. Diagram of cyroembedding and cyrosectioning procedures

immersion objective in conjunction with an Optronics Engineering CCD camera (Model No. DEI-470F) and color video monitor (Sony Corporation Model No. PVM-1342Q). An image of the stage micrometer was taken at these microscope settings to quantify biofilm thickness. The images were converted to a TIF file format and imported to *ImageTool*, (Version 2.0). Analysis was performed on a Digital Pentium® 133Mhz computer using the UTHSCSA *ImageTool* program (developed at the University of Texas Health Science Center at San Antonio, Texas and available from the Internet by anonymous FTP from maxrad6.uthscsa.edu with an Internet web address of <http://ddsdx.uthscsa.edu/dig/itdesc.html>). Twenty-one regions were arbitrarily chosen for measurement of biofilm thickness along the length of a sectioned sample. The sample was scanned a second time to acquire the minimum and maximum thickness. This software allows the user to define the substratum with a line and then perpendicularly move to the outer fringe of the biofilm. The measurement is displayed and stored in a spreadsheet format.

RESULTS

This section presents the results of experimental investigation into the efficacy of the antimicrobial agent, glutaraldehyde, and inhibitory agent, nitrite, on an indigenous population of sulfidogenic bacteria that was obtained from an oilfield produced water facility. Glutaraldehyde microbial experiments were conducted with both planktonic and biofilm cultures while the nitrite study was limited to the biofilm setting.

Planktonic Experiments

The undefined inoculum from the Lost Hills produced water facility was cultured for lactate utilizing sulfate-reducing bacteria using the Postgate C medium. The generation of sulfide and the corresponding uptake of sulfate by these microorganisms in batch vials over a 36-hour period are reported in Figure 6. Sulfide and sulfate concentrations are expressed in terms of mg-Sulfur/liter, e.g. 50 mg S²⁻ as S/L and henceforth are represented as mg-S/L. Sulfate levels were reduced by approximately 50% from their initial values. Using the same November 18, 1998 data and plotting the change in sulfide concentration versus change in sulfate concentration yielded a linear relationship with a correlation coefficient of 0.988 (Appendix E). As a precursor to the planktonic biocide experiments, batch vial studies were performed to document and address any potential changes in

activity or growth by monitoring the concentrations of sulfate and sulfide. Three pseudo-growth curves were performed and they are listed accordingly in Appendix E. An apparent specific growth rate was calculated from each of the sulfide curves, which ranged from 0.26 to 0.27 hr⁻¹. These rates were determined under growth conditions using the full strength Postgate C medium.

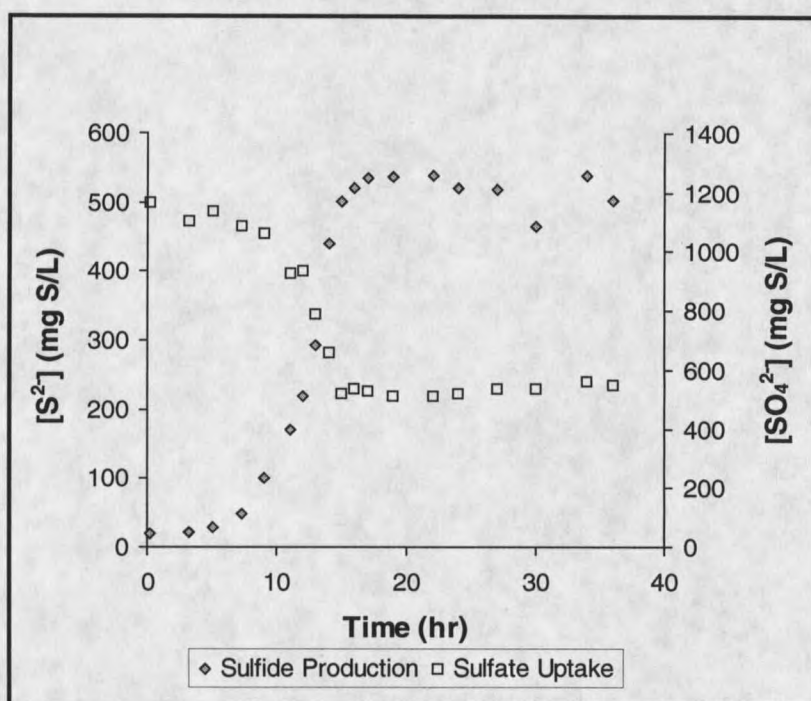


Figure 6. Sulfide production and sulfate uptake for a planktonic suspension enriched with Postgate C medium at 36°C (November 18, 1998 data).

The effectiveness of glutaraldehyde on planktonic SRB suspensions was determined by evaluating various concentrations of the biocide (0, 50, 100, 350, and 500 mg/L) on a viable 16-hour culture. Treatment efficacy was assessed by the period of sulfide inhibition. The delivery of the biocide coincided with the

microorganisms departure from the exponential phase of their growth.

Figure 7 depicts the recovery in the microorganisms ability to reduce sulfate as a function of glutaraldehyde concentration. As can be observed, concentrations of ≥ 100 mg/L were lethal to the planktonic suspensions. A portion of the exponential growth phase for the 50 mg/L vial was unfortunately not captured due to the abrupt resumption in sulfide production.

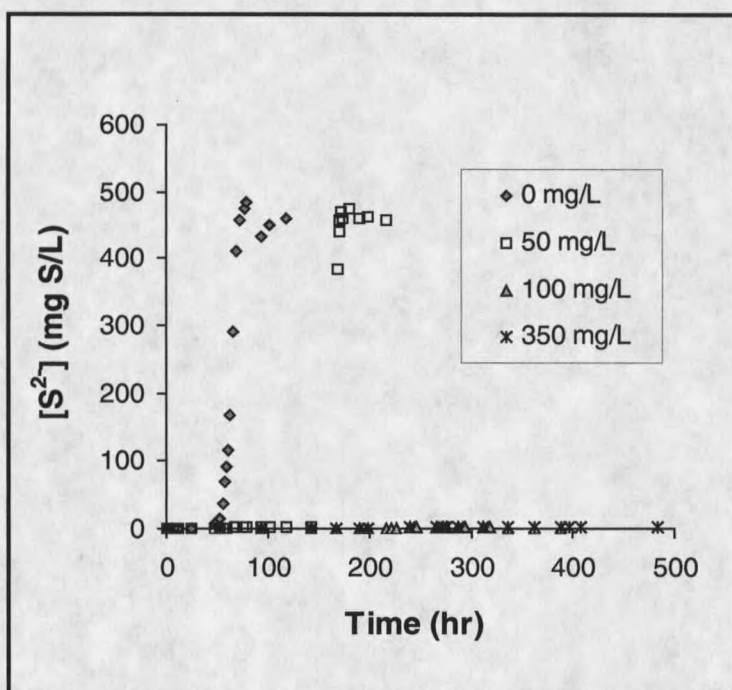


Figure 7. Effect of glutaraldehyde on the activity of planktonic sulfate-reducing bacteria. (Planktonic Experiment #1)

The results presented in Figure 7 were also interpreted in terms of two measurable parameters. The first entity was the amount of time metabolic activity was suppressed below 10 mg-S/L of produced sulfide ($t_{<10 \text{ mg-S/L}}$). A similar quantitative analysis was expressed in terms of the time required to attain 90% of pretreatment steady-state sulfide levels ($t_{90\% \text{ S-S}}$). The respective quantities for these measurables from the planktonic experiments are listed in Table 4.

Table 4. Planktonic recovery time in response to glutaraldehyde treatment. Recovery indices are expressed in terms of the time sulfide production is suppressed below 10 mg-S/L and the time required to reach 90% of steady-state sulfide levels. Recovery time was measured beginning at the time when fresh nutrients were supplied to the vials.

Glutaraldehyde Concentration	$t_{<10 \text{ mg-S/L}}$ (hr)	$t_{90\% \text{ S-S}}$ (hr)
0 mg/L #1	49	69
0 mg/L #2	49	65
0 mg/L #3	42	57
50 mg/L	143	169
100 mg/L	>385	>385

The 50 mg/L level of glutaraldehyde rendered approximately a 100-hr delay as compared to the control vial (0 mg/L glutaraldehyde) for both the time below 10 mg-S/L of sulfide and the time in obtaining 90% of steady-state sulfide levels. Activity in the 100 mg/L was monitored in excess of 385 hours with no evidence of recovery in sulfide production. The planktonic laboratory data and sulfide recovery times are listed in Appendices E and I, respectively.

Biofilm Experiments

Biofilm Reactor Mixing Characteristics

The hydraulic character of a process reactor can be defined by the residence time distribution of individual particles of liquid flowing through the tank (Viessman and Hammer, 1993). The ultimate goal in defining the hydraulic characteristics of the annular reactor was to provide a better approximation for predicting reactive behavior of constituents in the reactor. Knowing the hydraulic residence time distribution (HRT) of a reactor and its degree of dispersion allows for the basis of developing a kinetic description of a process reaction.

A tracer study was used to evaluate the HRT in the rotating annular reactor by introducing a slug of red food coloring into the reactor influent while measuring its effluent concentration over time. This pulsed injection of the non-reactive tracer study was repeated four times with the BioSurface Technologies Model 920 Biofilm Annular Reactor. Two of these evaluations addressed mixing differences as a function of the influent port orientation, i.e. top versus bottom feed, with minimal discrepancies between the studies. The remaining experiments were duplicate bottom feed studies operated at an inner cylinder rotational speed of 150 rpm and an influent flow rate of 7.9 ml/min. The compiled parameter analyses for the bottom feed experiment data sets are listed in Table 5 where Q is the flow rate

(mL/min), V_R the reactor volume (mL), D the dilution rate (hr^{-1}), and t_m the mean hydraulic residence time (hr).

Table 5. Hydraulic characteristics of non-reactive tracer studies.

Parameter	Bottom Feed Experiments		
	Theoretical	Tracer #3	Tracer #4
Q (mL/min)	7.9	7.9	7.9
V_R (mL)	1000	985	1030
D (hr^{-1})	0.5	0.47 ± 0.001	0.43 ± 0.002
t_m (min)	120	125	130

The effluent concentration profile (C curve) in Figure 8 illustrates the effluent response to the pulsed influent stimulus.

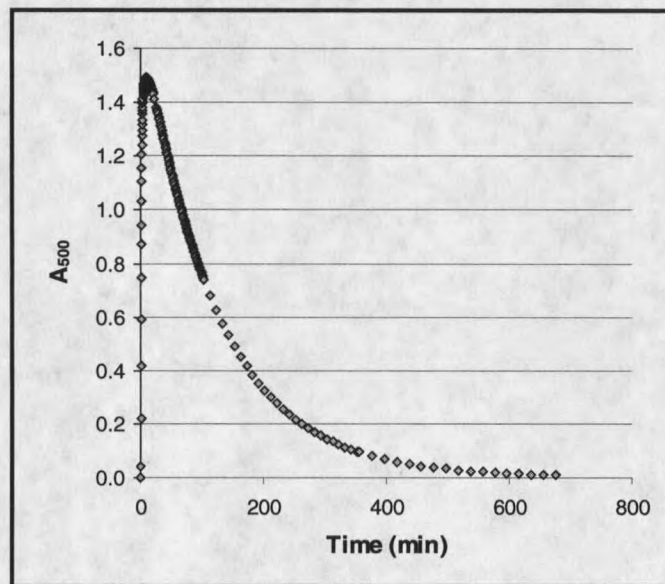


Figure 8. Effluent concentration profile from Tracer #3 for a bottom feed to the annular reactor. The reactor was operated at 150 rpm with an influent flow rate of 7.9 mL/min.

The washout behavior in an ideal CSTR can be modeled by an exponential decay function or by performing a natural logarithm transformation of the effluent concentration and plotting versus time. The slope of the linear regression represents the dilution rate for the reactor in the absence of reactive constituents. This concept is further illustrated in Figure 9 with all the associated analyses and experimental data listed in Appendices B and C.

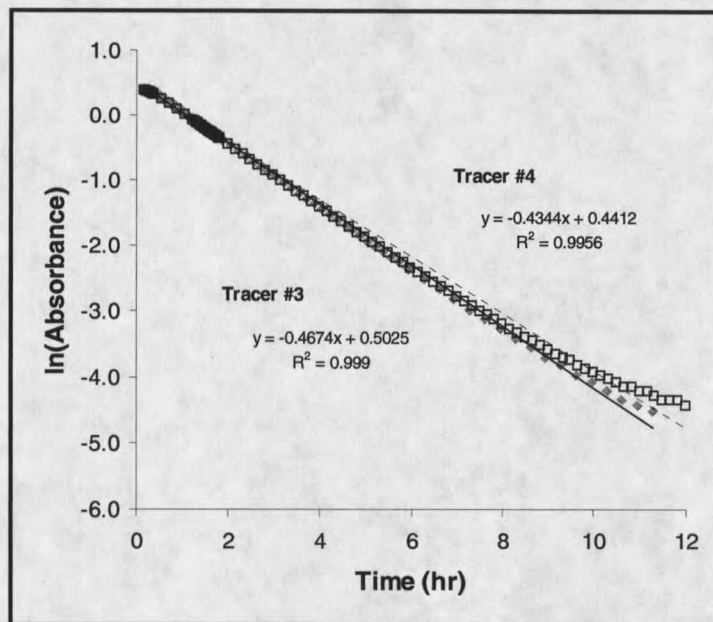


Figure 9. Washout behavior (slope = dilution rate, D) of the non-reactive tracer in the BST Model 920 biofilm annular reactor.

Sequence of Events for Biofilm Experiments

One of the mechanisms for glutaraldehyde's efficacious nature with microorganisms is the biocide interaction with membrane bound protein (Scott and

Gorman, 1991). Yeast extract was one of the Postgate C medium components that obviously possess inherent cellular components. To prevent neutralization of the glutaraldehyde by the Postgate C medium, the medium was "flushed" from the reactor prior to administering the biocide. Table 6 categorizes the sequence of events required for the dosing with glutaraldehyde. This protocol is portrayed in Figure 10 for a given biofilm annular reactor experiment through the aid of the biogenic sulfide profile. The data points are connected to assist the reader with interval transitions.

The rotating annular reactor was operated in batch mode until a steady-state sulfide level of approximately 50 mg-S/L was achieved. As the reactor was transferred from batch to continuous flow, the produced sulfide was displaced from the reactor. Microbial sulfide production resumed as the microorganisms began to metabolize the replenished carbon and energy sources. Washout of sulfide and sulfate occurred during the medium "flush" stage of the protocol to diminish the neutralization effects of the medium with the biocide. The nutrient amendment was reinstated after the biocide treatment period. Metabolic activity was again evident through the assimilation of sulfate and the corresponding production of sulfide.

Table 6. Biofilm annular reactor biocide dosing sequence protocol

Sequence	Event	Description
1	Batch Mode	~48 hours to steady-state $[S^{2-}] = 50$ mg-S/L
2	CSTR Mode	Initiate continuous flow, washout, and recovery
3	Steady state	$[S^{2-}] = 50+$ mg-S/L
4	Medium flush	Elimination of abiotic reaction of biocide and medium
5	Biocide treatment	Pulse dose injection of concentrated biocide
6	Contact period	6.75 hour monitoring of biocide and metabolic activity
7	Resume medium flow	Nutrient flow restarted; sulfate replenished and sulfide levels monitored
8	Steady-state	Sulfide levels return to approximately 50 mg-S/L

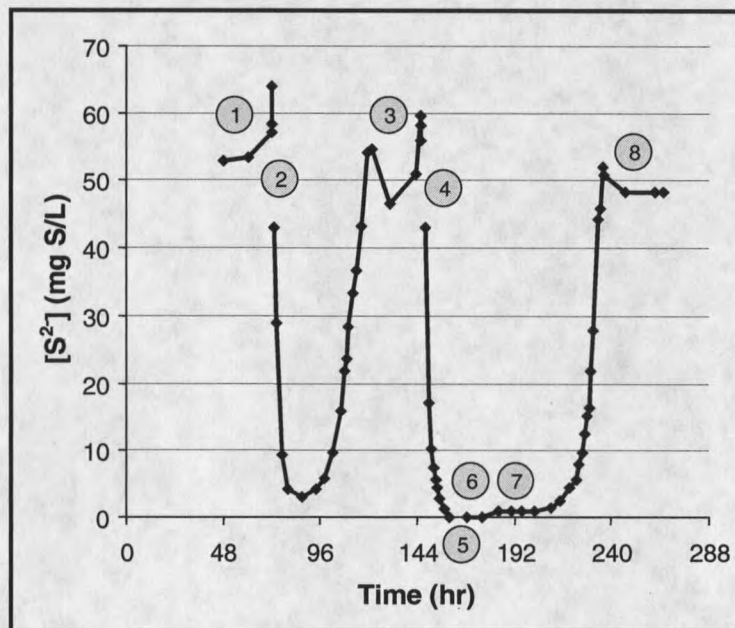


Figure 10. Sequence of events during a biofilm experiment (Experiment #8). The numbers correspond to the steps summarized in Table 6.

Control Experiments

The control experiments proceeded in the same fashion as the biocide studies but with one important difference. The applied dose was a 1-mL pulse injection of ultrapure water. The nutrient medium "flush" stages commenced after approximately 24-30 hours of pretreatment steady-state sulfide levels. Figure 11 exemplifies the sulfide and sulfate profiles for a typical repetitive control dose experiment.

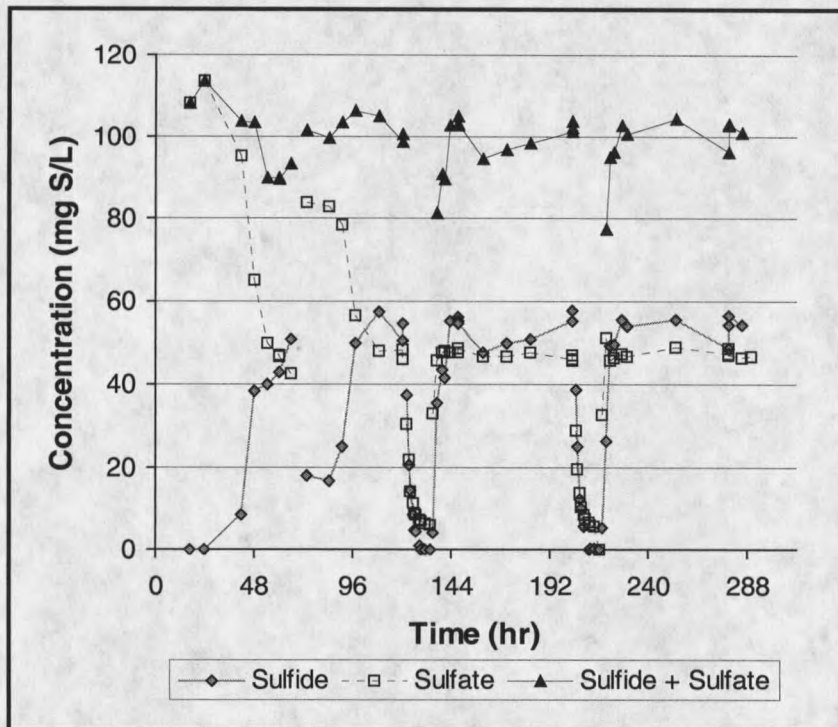


Figure 11. Typical annular reactor control experiment. Concentration profiles for sulfide and sulfate in response to a repetitive dose with ultrapure water. See Table 6 and Figure 10 for experimental protocol. (Control #3 data)

The plot of the total sulfur (sulfide plus sulfate) for the system qualitatively illustrated near closure of the mass balance. It was hypothesized the remaining

sulfur was bound in terms of a FeS precipitate. The sulfide profile portrayed the sequence outlined in the preceding section. As the nutrient flow was returned to the reactor environment, a similar and immediate response in sulfate reduction was observed for two independent doses.

Comparison of Control Experiments

Two control experiments were performed in the annular reactor. One application was a single dose while the second study investigated the response to a repetitive dose of ultrapure water. The 1/10th strength Postgate C medium was delivered to the reactor, which provided an available electron donor concentration of approximately 100 mg-S/L as sulfate. These two experiments were performed to demonstrate the reproducibility of the annular reactor while obtaining a baseline of microbial activity. Since these experiments were not subjected to any inhibitory or biocidal agents, the combined profiles from the two experiments were interpreted as a triplicate of single ultrapure water doses. The complementary profiles of sulfide and sulfate for the three individual dosing periods are shown in Figure 12. These profiles exemplified good repeatability between experiments. In the case of the sulfate curves, the sulfate-reducing bacteria from Control #2 displayed a 3-hour delay in metabolizing the sulfate as compared to the microorganisms for the two profiles from Control #3. The last sampling point of the steady-state intervals was performed in either duplicate or triplicate to document potential sampling variation. The experimental data for these studies

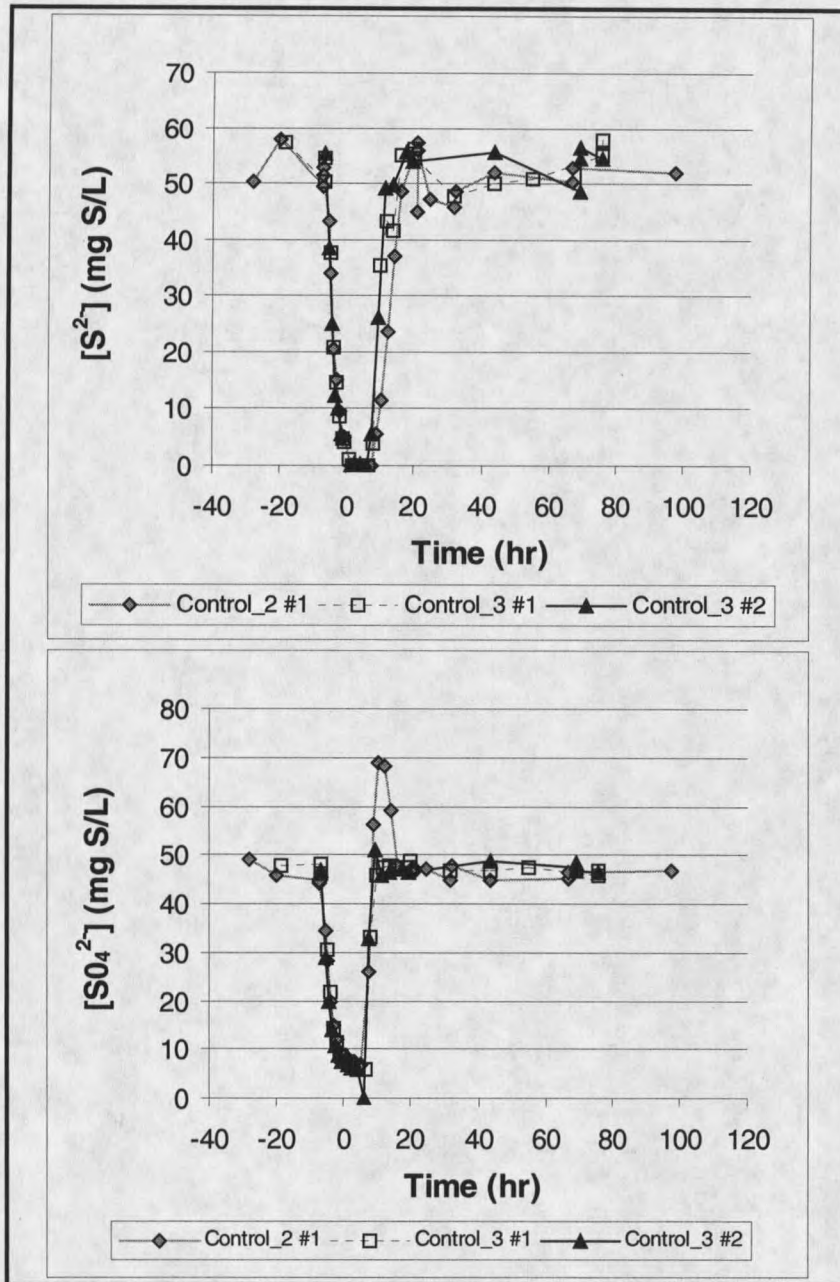


Figure 12. Sulfide and sulfate profile comparison for annular reactor control experiments administered with a 1-mL dose of ultrapure water. The notation #1 implies dose #1 and #2, dose #2. Time zero denotes the pulse injection of ultrapure water; $-6.5hr$ the time nutrient amendment ceased; and $+7hr$ the time nutrient amendment was reinitiated.

are listed in Appendix F.

Biocide Experiments

A 1-mL pulse injection of concentrated glutaraldehyde was administered to provide a calculated peak concentration of 500 mg/L. Three separate experiments were performed: one single dose and two repetitive dose studies. This provided an overall comparison of three single doses with a similar evaluation between the two repetitive dose profiles. The raw data for the biofilm experiments are listed in Appendices F through I.

Figure 13 demonstrates the changes in the metabolic activity of the sulfate-reducing bacteria as a result of a repetitive biocide dosing scheme in the biofilm annular reactor. The figure illustrates the complimentary behavior between the production of sulfide and sulfate consumption during the respective periods of inhibition and recovery. Figure 14 portrays the sulfide profile comparison for the three separate experiments with time zero indicating the pulse injection of the biocide.

Sulfide production was inhibited for similar periods in each of the glutaraldehyde dosing experiments. At first glance, Experiment #4 appears to return to steady-state values that are lower than the pretreatment sulfide levels. Further review of the raw data revealed the average pre- and post-dose concentrations are within 2%. The pre-dose interval displayed two initial sampling

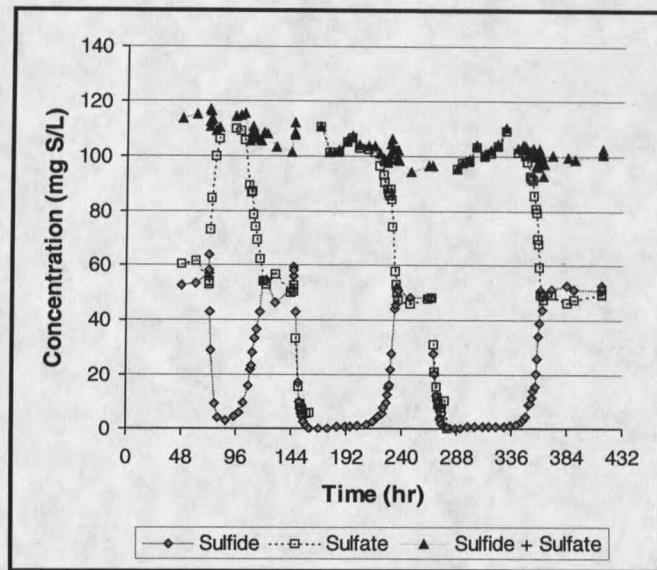


Figure 13. Sulfide and sulfate concentration profiles in response to repetitive pulse injections of 500 mg/L glutaraldehyde. See Table 6 and Figure 10 for experimental protocol. (Annular reactor Experiment #8 data)

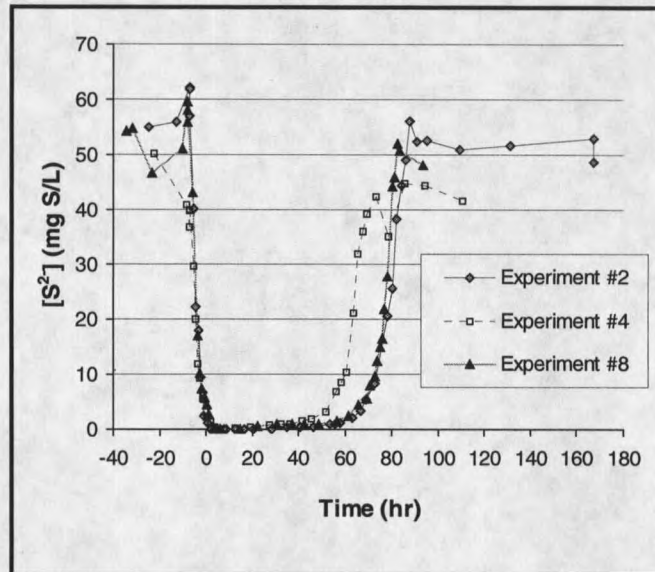


Figure 14. Sulfide profile comparison for three separate annular reactor experiments that were subjected to a single dose of 500 mg/L glutaraldehyde. Time zero denotes the pulse injection of glutaraldehyde; -6.5hr the nutrient ceased; and $+7\text{hr}$ was reinitiated.

points that exceeded 50 mg-S/L of sulfide with four additional samples that bordered concentrations of 40 mg-S/L.

Polycarbonate coupons were sampled at discrete intervals to ascertain biofilm thickness and areal carbon density. The corresponding sets of coupon data are listed in Appendices G and H, respectively, with the mean values and standard deviations similarly reported in Tables 12 and 13 of the Biofilm Thickness and Areal Carbon Density sections.

Glutaraldehyde and Control Dosing Comparison

The sulfide profiles in Figure 15 depict the behavior consistent with washout due to medium removal, suppression during the dosing interval, and obvious resurgence of the sulfate-reducing bacteria. It was apparent that the Experiment #2 profile (glutaraldehyde treatment) experienced a period of suppressed sulfide production after resumed nutrient flow when compared to the control.

An alternative representation of glutaraldehyde efficacy was summarized in Table 7. The associated raw data are located in Appendix I. As illustrated, the Control biofilms were restored to 90% of their pretreatment steady-state sulfide levels in fewer than 10 hours. The biofilms subjected to the glutaraldehyde treatments were consistently suppressed below 10 mg-S/L of sulfide for a period of 60.8 ± 10.8 hours post continuation of nutrient flow. These treated biofilms achieved 90% of steady-state in an average of 72.6 ± 8.7 hours in contrast to

7.3 ± 2.1 hours for the Control studies. Both the control and treatment experiments exemplified a more rapid resurgence when compared to their initial continuous flow profile.

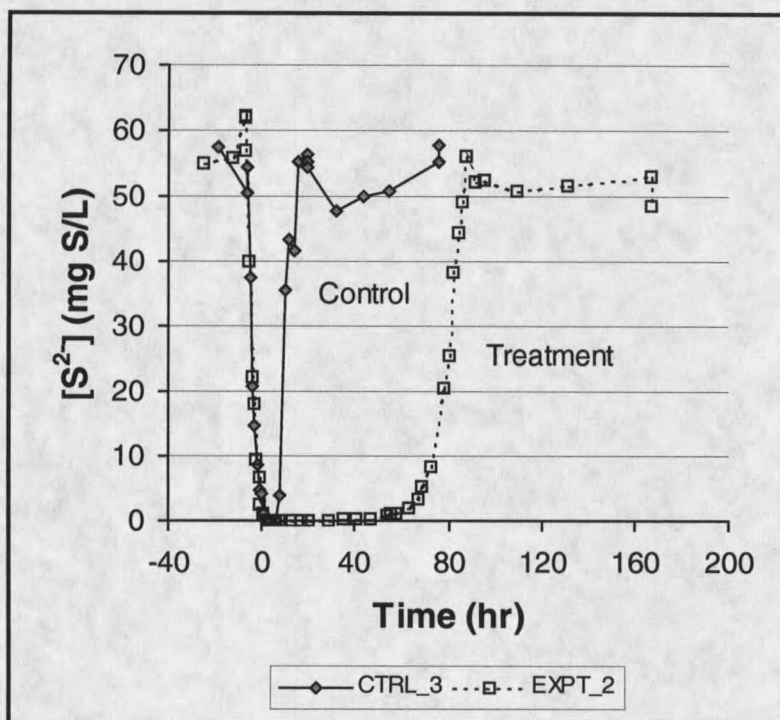


Figure 15. Sulfide profile comparison between a control experiment with ultrapure water versus a dose of 500 mg/L glutaraldehyde. Time zero denotes the pulse injection of glutaraldehyde; $-6.5hr$ the time nutrient amendment ceased; and $+7hr$ the time nutrient amendment was reinitiated. (Annular reactor data from Control #3 and Experiment #2)

Table 7. Sulfate-reducing bacterial biofilm recovery time in response to glutaraldehyde treatments. Recovery indices are expressed in terms of the time sulfide production is suppressed below 10 mg-S/L and the time required to reach 90% of steady-state sulfide levels. Recovery time was measured beginning at the time when the nutrient amendment was reinitiated.

Annular Reactor Experiment	$t_{<10 \text{ mg-S/L}}$ (hr)	$t_{90\% \text{ S-S}}$ (hr)
Control_2	3	9
Control_3 #1	1	8
Control_3 #2	1	5
Experiment_2	67	80
Experiment_4 #1	53	65
Experiment_4 #2	46	62
Experiment_8 #1	66	75
Experiment_8 #2	72	81

Glutaraldehyde Reaction Rates

Retrieval of aqueous samples for the quantification of glutaraldehyde levels within the annular reactor commenced one minute following biocide injection. Samples were acquired every fifteen minutes during the 6.75-hour contact period. The bulk liquid biocide concentration for the dosing cycle followed an exponential decay profile similar to the effluent profiles for the non-reactive tracer studies.

An overall objective of the biocide studies was to gain insight to the behavior of the biofilm when it was subjected to the dosing of the antimicrobial agent, glutaraldehyde. Therefore, it was of interest to examine the possibility and to what

extent the biofilm would react with the biocide. A conventional reaction kinetics approach to such an interaction is to initially perform a natural logarithm transformation of the concentration data and plot these values versus time. This analysis is portrayed in Figure 16 for the individual doses of glutaraldehyde. The distribution of the data exhibit similar linear transformations. Values of the correlation coefficient for the linear fit to the data sets exceed 0.99. The corresponding transformations and regression analyses are listed in Appendix J.

The slope of these curves is a composite first-order reaction rate coefficient, K , which is characterized by reactor hydraulics and the interaction of the biocide with the biofilm. The values are listed in Table 8. The mean value of this rate coefficient for the five independent doses is 0.43 hr^{-1} . Embedded within the value of slope are the dilution rate, D , and the biocide reaction rate coefficient, k .

Performing a glutaraldehyde mass balance with respect to the annular reactor control volume provides a mechanism for determining the reaction rate coefficient. For the bulk fluid phase of interest, the mass balance incorporates accumulation, bulk flow in and out of the reactor, and the surface reaction of the biocide with the biomass within the reactor. The governing mass balance proceeds as follows.

$$\text{Accumulation} = \text{Flow In} - \text{Flow Out} - \text{Reaction} \quad (1)$$

Since glutaraldehyde was not a component of the influent feed to the reactor, the second term reduces to zero. Substituting the parameters that describe the remaining processes results in equation (2).

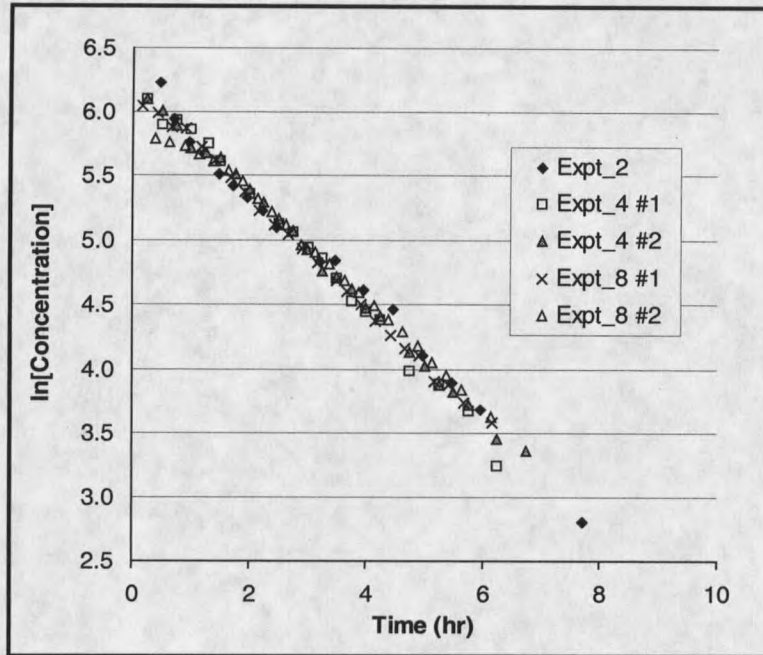


Figure 16. Natural logarithm of the glutaraldehyde concentration versus time for all glutaraldehyde annular reactor experiments. The slope of these curves provides the first order reaction rate coefficients of the glutaraldehyde.

Table 8. Composite first-order reaction rate coefficients for the glutaraldehyde annular reactor experiments.

Glutaraldehyde Study	K (hr^{-1})
Experiment_2	0.43
Experiment_4 #1	0.46
Experiment_4 #2	0.44
Experiment_8 #1	0.43
Experiment_8 #2	0.40

$$V \frac{dC_B}{dt} = -QC_B - r_B A_b L_f \quad (2)$$

where V is the reactor volume (m^3), C_B the biocide concentration (mg/m^3), Q the flow rate (m^3/sec), r_B the reaction rate of glutaraldehyde with the biofilm ($mg/m^3 \cdot hr$), A_b the biofilm surface area (m^2), and L_f the biofilm thickness (m). Since the natural logarithm transformation of the biocide concentration versus time data yields a first-order dependence; the reaction rate was defined as

$$r_B = kC_B \quad (3)$$

with k termed the first-order reaction rate coefficient (hr^{-1}). Substituting (3) into (2) and rearranging the relationship results in the expression described by equation (4).

$$\frac{dC_B}{C_B} = - \left[\frac{Q}{V} + \frac{kA_b L_f}{V} \right] \quad (4)$$

The term Q/V is defined as the dilution rate, D . Integration of equation (4) produces

$$\ln \left(\frac{C_B}{C_{Bi}} \right) = e^{- \left[D + \frac{kA_b L_f}{V} \right]} \quad (5)$$

where C_{Bi} is the initial biocide concentration and the exponent is described by the slope of the $\ln C_B$ vs. *time* curve (previously defined as the composite reaction rate coefficient, K). Solving for the reaction rate coefficient results in equation (6).

$$k = \frac{V}{A_b L_f} (K - D) \quad (6)$$

The individual reaction rate coefficients are summarized in Table 9. The calculations utilized an average biofilm thickness (post biocide dose, Table 11), a reactor surface area of 0.26 m² (Appendix A), a dilution rate of 0.43 hr⁻¹, and a nominal reactor volume of 1-L. The dilution rate was lower than the tracer study values because the overall flow rate was reduced in the absence of the nutrient medium flow to the reactor.

Table 9. First-order reaction rate coefficients for the glutaraldehyde annular reactor experiments.

Glutaraldehyde Study	$L_{f\text{ avg}}$ (μm)	K (hr ⁻¹)	k_{glut} (hr ⁻¹)
Experiment_2	5.1	0.43	0
Experiment_4 #1	5.7	0.46	20
Experiment_4 #2	4.4	0.44	8.7
Experiment_8 #1	3.1	0.43	0
Experiment_8 #2	5.8	0.40	0

It was stated previously that the tracer studies elucidated the behavior of a non-reactive species traveling through the reactor, i.e. the dilution rate. The maximum difference between the dilution rate for the two tracer studies and the lowest composite glutaraldehyde reaction rate coefficient was 0.03 hr⁻¹.

Nitrite Addition

Inhibition of microbial produced sulfide was also investigated by introducing a 24-hour continuous dose of approximately 110 mg-N/L of nitrite to the rotating annular reactor. The time course of sulfide production proceeded with a similar protocol to the glutaraldehyde studies except the nutrient flow was maintained during the delivery of the nitrite to potentially elicit a sulfide production response.

The nitrite was added with the 1.5% NaCl dilution water after 30 hours of steady-state sulfide levels. Within 30 minutes and as long the nitrite levels exceeded 15 mg-N/L; the produced sulfide levels started to decrease. The nitrite concentration attained 100 mg-N/L in the bulk liquid after 6-hours of continuous feed. This coincided with a sulfide level of approximately 4 mg-S/L. The sulfate concentrations during this dosing period corroborated the sulfide levels, which indicated inhibition of SRB metabolism. The changes in nitrite, sulfide and sulfate concentrations are illustrated in Figure 17 for the 110 mg-N/L nitrite repetitive dose. The experimental data for this study are listed in Appendix F. The time to recovery commenced when the nitrite flow was removed from the biofilm reactor. Four hours after the nitrite delivery was terminated, the bulk fluid nitrite levels were less than 15 mg-N/L and resuscitation in sulfide production was noted. As residual nitrite was flushed from the reactor, microbial produced sulfide was no longer suppressed.

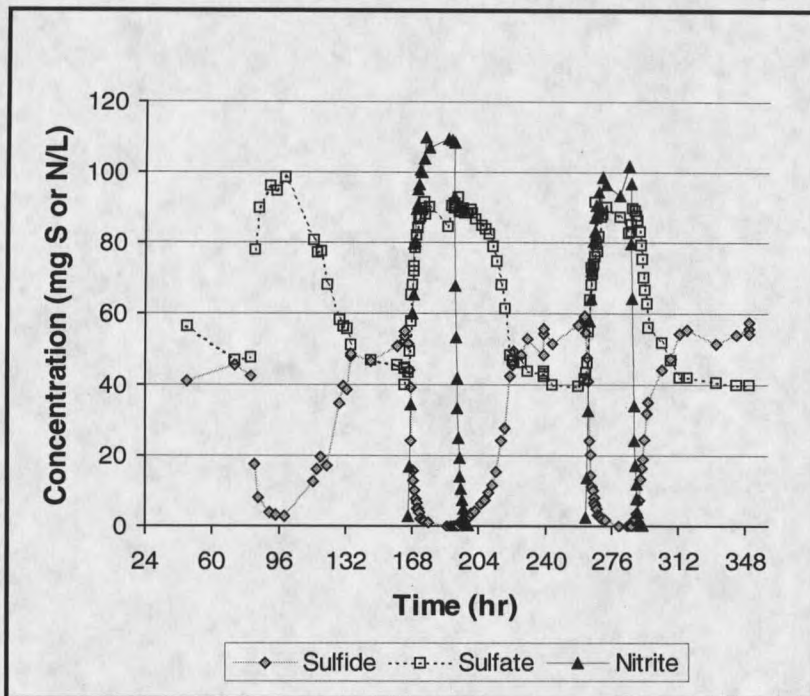


Figure 17. Sulfide and sulfate concentration profiles in response to two 24-hour continuous feeds of 110 mg-N/L of nitrite. See Table 6 and Figure 10 for experimental protocol. (Annular reactor Experiment #6 data)

The repetitive dose rendered similar results: repressed sulfide levels after 30 minutes of exposure to the nitrite (bulk liquid nitrite concentration of 14 mg-N/L). Sulfide levels decreased to 4-5 mg-S/L with a bulk fluid nitrite concentration of 90 mg-N/L as compared to 100 mg-N/L for the first dose. Sulfate levels confirmed the inhibition of sulfide with the bulk liquid concentration being equal to the influent levels. The recovery of sulfide production occurred earlier with the second dose, Table 10, as evident by sulfide levels approaching 2 mg-S/L only two hours after terminating the nitrite delivery. This was coincident with 33 mg-N/L nitrite in the

bulk fluid. It was also noted that the bulk fluid nitrite concentration during the second dosing interval never exceeded 102 mg-N/L as compared to 110 mg-N/L for the first application. The influent nitrite concentration throughout the individual doses averaged 112 mg-N/L.

Table 10. Sulfate-reducing bacterial biofilm recovery time in response to nitrite addition. Recovery indices are expressed in terms of the time sulfide production is suppressed below 10 mg-S/L and the time required to reach 90% of steady-state sulfide levels. Recovery time was measured beginning at the time when the nutrient amendment was reinitiated.

Nitrite Experiment & Dose	$t_{<10 \text{ mg-S/L}}$ (hr)	$t_{90\% \text{ S-S}}$ (hr)
Experiment_6 #1	19	32
Experiment_6 #2	5	24

The washout behavior of the nitrite from the rotating annular reactor for the two doses is illustrated in Figure 18. Qualitatively, the nitrite washout profiles appear to be nearly identical. Further examination revealed the residual from the second dosing period was removed 1.5 hours earlier than the first dose. These two curves demonstrate a faster departure from the reactor when compared with exit age distribution for one of the glutaraldehyde experiments.

As with the analysis of the glutaraldehyde data, a natural logarithm transformation of the concentration versus time data was made to gain insight to the reaction kinetics between the nitrite and biofilm during the washout phase. The converted data sets are plotted in Figure 19. Transformations were not performed

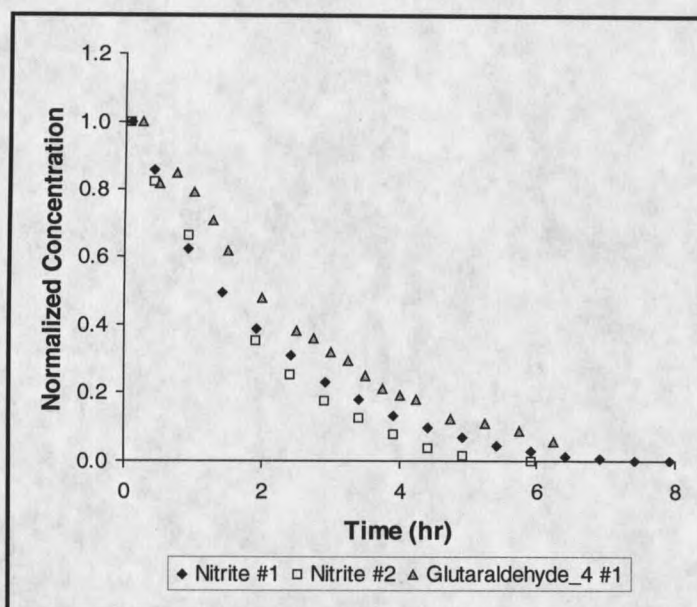


Figure 18. Comparison of nitrite and glutaraldehyde washout profiles from the biofilm annular reactor.

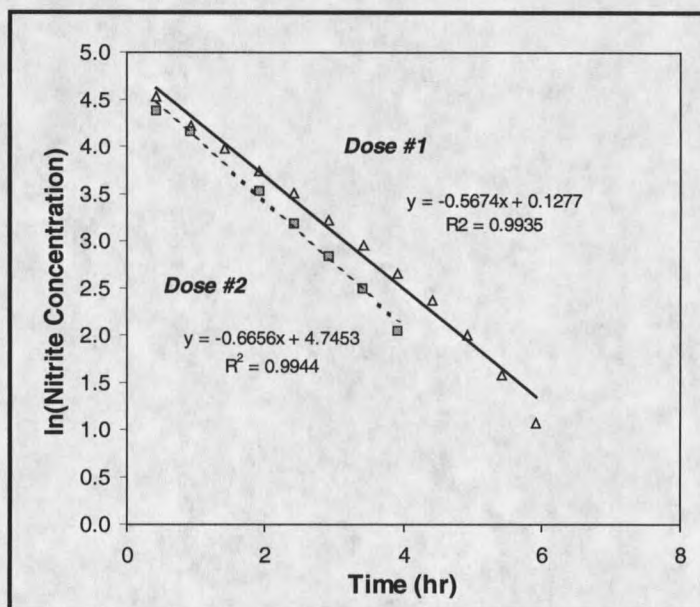


Figure 19. Natural logarithm of nitrite concentration versus time for two separate doses in annular reactor Experiment #6. The slope of these curves provides the first-order reaction rate coefficients during washout.

for nitrite concentrations that were less than 1 mg-N/L. There was a good correlation of the linear fit to the data with r^2 values exceeding 0.99. Correlation by the use of a linear transformation implied a first-order reaction rate coefficient, which was designated by the slope of the curve. The reaction rate coefficients for the effluent portion of the dosing cycle were 0.57 and 0.67 hr^{-1} , respectively for the first and second doses. The coefficients were greater than the dilution rate of the reactor (0.5 hr^{-1}) which indicated a reaction between nitrite and the microorganisms as nitrite was displaced from the reactor environment.

A more important aspect was the reaction rate of the nitrite during the dosing cycle. The material balance again provides a phenomenological approach in determining the observable reaction rate. The balance for the bulk liquid phase begins with the processes of accumulation, flow in, flow out, and the reactive component. The accumulation term was reduced to zero since the analysis was concurrent with steady-state influent and bulk liquid levels of nitrite. Equation (7) portrays the simplified material balance for the nitrite.

$$Q(C_{in,avg} - C_{out,avg}) = R_{obs} A_b L_f \quad (7)$$

The observed reaction rate was therefore described by

$$R_{obs} = \frac{Q(C_{in,avg} - C_{out,avg})}{A_b L_f} \quad (8)$$

The steady-state nitrite concentrations were averaged over the last five sampling points of the interval and the reactor flow rate was operated at 7.9 mL/min. The

average thickness of the biofilm post the dosing periods was used in the evaluation of equation (8). Table 11 lists the observable rates for these two nitrite doses.

Table 11. Observable reaction rate for nitrite doses.

Nitrite Dose	$C_{in,avg}$ (mg/L)	$C_{out,avg}$ (mg/L)	$L_{f,avg}$ (μm)	R_{obs} (mg/L*min)
1	112.4	107.9	4.7	29.3
2	112.5	95.7	9.9	51.7

Biofilm Coupon Analyses

Biofilm Thickness

Utilization of the cryoembedding and cryosectioning techniques permitted assessment of biofilm cross-sections with resolution capability to individual bacterial cells. Epifluorescent microscopic examination of the embedded biofilm revealed a heterogeneous structure that consisted of microcolonies, potential water channels, and occasional aggregated structures. Biofilm thickness varied during the course of an experiment as a result of the different dosing protocol sequences. Forty-nine discrete measurements (7 measurements/image) were captured on a per coupon basis with the average thickness and standard deviation reported in Table 12. Data for the individual experiments are listed in Appendix I. The data in the table substantiate the qualitative observations made with regards

Table 12. Biofilm thickness, L_f

Experiment	Interval	L_f (μm)		
		Min	Max	$\bar{X} \pm \sigma$
<i>Control #2</i>	Steady-state	0.0	17.7	2.9 ± 2.1
	Before dose	0.0	23.7	2.4 ± 1.9
	After dose	0.0	15.9	3.6 ± 2.0
	Return to steady-state	3.8	10.9	4.0 ± 2.6
<i>Control #3</i>	Steady-state	0.0	32.4	4.5 ± 2.5
	Before dose #1	0.0	33.9	5.9 ± 6.5
	Return to steady-state	0.0	21.7	5.2 ± 2.0
	Before dose #2	0.0	14.0	6.2 ± 2.6
	Return to steady-state	0.0	24.2	8.0 ± 3.9
<i>Experiment #2</i>	Steady-state	1.7	25.4	8.2 ± 3.5
	After dose	0.0	17.3	5.1 ± 2.4
	Return to steady-state	0.0	23.5	7.4 ± 4.2
<i>Experiment #4</i>	Steady-state	0.0	19.6	2.4 ± 1.6
	After dose #1	0.0	26.9	5.7 ± 3.8
	Return to steady-state	0.0	25.0	5.9 ± 3.9
	After dose #2	0.0	18.3	4.4 ± 3.0
	Return to steady-state	0.0	34.8	9.8 ± 5.4
<i>Experiment #6</i>	Steady-state	0.0	22.3	4.5 ± 2.2
	After dose #1	0.0	12.3	4.7 ± 2.6
	Return to steady-state	0.0	31.2	6.8 ± 4.4
	After dose #2	0.0	35.1	9.9 ± 6.1
	Return to steady-state	0.0	41.1	10.0 ± 6.8
<i>Experiment #8</i>	Steady-state	0.0	49.1	6.8 ± 5.6
	After dose #1	0.0	31.7	3.1 ± 4.1
	Return to steady-state	0.0	26.2	5.8 ± 2.6
	After dose #2	0.0	32.6	5.8 ± 3.5
	Return to steady-state	0.0	40.9	10.2 ± 4.5

